

Supporting Information (SI)

**Synthesis and Exceptional Operational Durability of Polyaniline-Inspired  
Conductive Ladder Polymers**

*Mingwan Leng<sup>1</sup>, Nandu Koripally<sup>3</sup>, Junjie Huang<sup>1</sup>, Aikaterini Vriza<sup>4</sup>, Kyeong Yeon Lee<sup>2</sup>,  
Xiaozhou Ji<sup>1</sup>, Chenxuan Li<sup>1</sup>, Megan Hays<sup>1</sup>, Qing Tu<sup>2</sup>, Kim Dunbar<sup>1</sup>, Jie Xu<sup>4\*</sup>, Tina Ng<sup>3\*</sup>, and  
Lei Fang,<sup>1,2\*</sup>*

<sup>1</sup> Department of Chemistry, Texas A&M University, College Station, TX 77843-3255, USA

<sup>2</sup> Department of Materials Science and Engineering, Texas A&M University, College Station,  
TX 77843-3255, USA

<sup>3</sup> Material Science and Engineering Program and Department of Electrical and Computer  
Engineering, University of California San Diego, La Jolla, California 92093, United States

<sup>4</sup> Nanoscience and Technology Division, Argonne National Laboratory, Lemont, Illinois  
60439, United States

Email: xuj@anl.gov; tnn046@ucsd.edu; fang@chem.tamu.edu

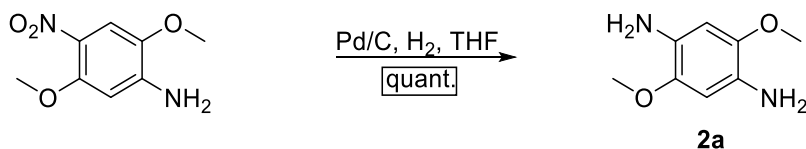
## TABLE OF CONTENTS

<b>1. General Method</b> .....	3
<b>2. Synthesis</b> .....	4
<b>3. Oxidation, Reduction, and Protonation Titration</b> .....	12
<b>4. Conductivity Optimization</b> .....	15
<b>6. Diradical Character Calculation</b> .....	21
<b>7. Cyclic voltammetry and Spectroelectrochemistry</b> .....	22
<b>8. Stability Measurement in 99% MSA</b> .....	24
<b>9. Electrochemical Stability Measurement</b> .....	25
<b>10. Galvanostatic charge-discharge curves (GCD) of Supercapacitor setup</b> .....	27
<b>11. Thermogravimetric Analysis (TGA)</b> .....	27
<b>12. X-ray Crystallography</b> .....	28
<b>13. Grazing-Incidence Wide-Angle X-Ray Scattering</b> .....	33
<b>14. NMR Spectra</b> .....	35
<b>15. Mass Spectra</b> .....	50

## 1. General Method

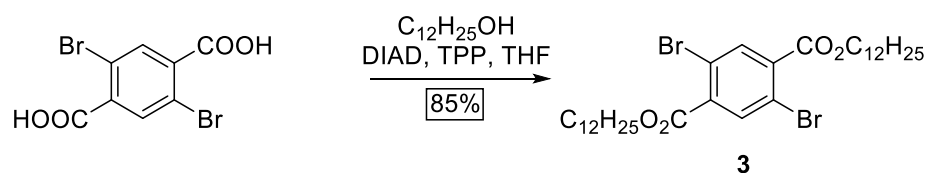
All reaction solvents were dried and purified by an Inert Technology pure solvent system (PureSolv-MD-5a). All starting materials were obtained from commercial suppliers and were used without further purification unless otherwise specified.  $^1\text{H}$ ,  $^{13}\text{C}$ ,  $^1\text{H}$ - $^{13}\text{C}$  HSQC and  $^1\text{H}$ - $^{13}\text{C}$  HMBC nuclear magnetic resonance (NMR) spectra were recorded on Bruker 400 MHz and 500 MHz spectrometer at room temperature and processed by MestReNova. Chemical shifts are reported in ppm relative to the signals corresponding to the residual non-deuterated solvents (for  $^1\text{H}$  NMR:  $\text{CD}_2\text{Cl}_2$   $\delta$  = 5.32 ppm;  $\text{CDCl}_3$   $\delta$  = 7.26 ppm;  $\text{THF-}d_8$   $\delta$  = 3.58 ppm;  $\text{DMSO-}d_6$   $\delta$  = 2.50 ppm; for  $^{13}\text{C}$  NMR:  $\text{CD}_2\text{Cl}_2$   $\delta$  = 53.84 ppm;  $\text{CDCl}_3$   $\delta$  = 77.16 ppm;  $d_8$ -THF  $\delta$  = 67.21, 25.31 ppm;  $\text{DMSO-}d_6$   $\delta$  = 39.52 ppm). Flash column chromatography purifications were carried out using a Biotage® Isolera™ Prime with various sizes of  $\text{SiO}_2$  Biotage SNAP® cartridges. Analytical size exclusive chromatography (SEC) was performed on a TOSOH EcoSEC (HLC-8320GPC) chromatography at 40 °C with UV detector at 254 nm and THF as the eluent. The molecular weights were calculated using a calibration curve based on the UV absorption signal of polystyrene standards. UV-Vis-NIR absorption spectra were recorded on a Hitachi U-4100 UV-Vis-NIR spectrophotometer. Atmospheric-pressure chemical ionization mass spectrometry (APCI-MS) experiments were performed using a Thermo Scientific Q-Exactive Focus operated in full MS in positive mode. FT-IR spectra were recorded in attenuated total reflectance mode (with ZnSe) using a Shimadzu IRAffinity-1S spectrometer. Cyclic Voltammetry (CV) and controlled potential experiments were performed with a Gamry Interface 1010 T potentiostat. Electron paramagnetic resonance (EPR) spectroscopy was conducted on a Bruker ELEXSYS II E500 with microwave frequency of ca. 9.38 GHz at 288 K.

## 2. Synthesis



**Scheme S1.** Synthesis of 2,5-dimethoxybenzene-1,4-diamine (**2a**) via reduction.

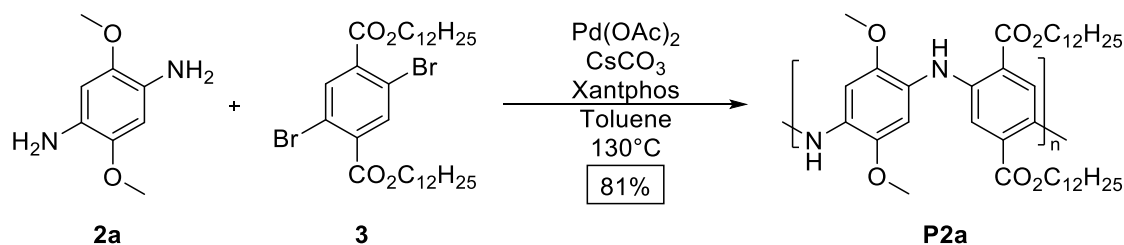
**2,5-dimethoxybenzene-1,4-diamine (2a):** **2a** was synthesized according to literature report<sup>1</sup>. 2,5-dimethoxy-4-nitroaniline (10.1 mmol, 2.0 g), Pd/C (10%, 1.20 mmol, 200.0 mg), and THF (10 mL) were added to a Schlenk flask. After the flask was degassed, a hydrogen gas balloon was attached. The mixture was stirred for 3 h at room temperature. The solution was then filtered and washed with THF to remove Pd/C. The solution was concentrated under vacuum to give the desired compound **2a** as a pale-yellow solid. <sup>1</sup>H NMR (400 MHz, DMSO-*d*<sub>6</sub>, 298 K) δ = 6.28 (s, 2H), 3.95 (s, 4H), 3.63 (s, 6H). <sup>13</sup>C NMR (100 MHz, DMSO-*d*<sub>6</sub>, 298 K) δ = 141.31, 128.05, 101.41, 56.30., HRMS (+APCI) calcd. [M+H]<sup>+</sup>: 169.0969 found: 169.0972.



**Scheme S2.** Synthesis of Didodecyl 2,5-dibromoterephthalate (**3**) via Mitsunobu reaction.

**Didodecyl 2,5-dibromoterephthalate (3):** **3** was synthesized according to literature report<sup>2</sup>. Under Nitrogen atmosphere, 2,5-dibromoterephthalic acid (20.0 mmol, 6.48 g), dodecanol (40.0 mmol, 7.64 g) and triphenylphosphine (TPP: 40.8 mmol, 10.70 g) in THF (150 mL) were added to a dried Schlenk flask. Diisopropyl azodicarboxylate (DIAD) (8.25 g, 40.8 mmol) was added slowly to the solution and stirred for 18 h at room temperature. The mixture was poured into a

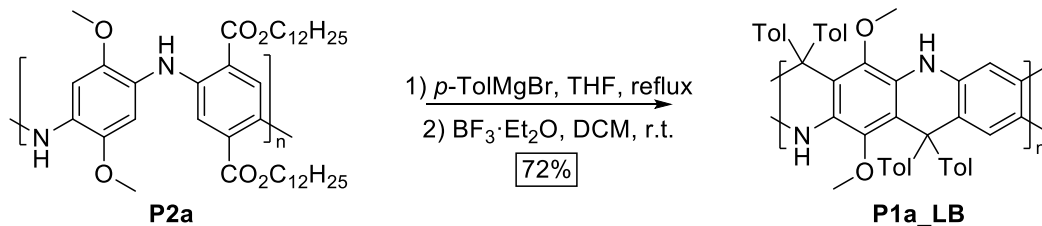
saturated aqueous solution of sodium bicarbonate (NaHCO<sub>3</sub>) and extracted with hexane, which was then washed with brine and water. The organic layer was dried over Na<sub>2</sub>SO<sub>4</sub> and filtered, and the solvent was evaporated. The product was further purified by recrystallization with hexane to give the desired compound **3** as a white solid. <sup>1</sup>H NMR (400 MHz, CDCl<sub>3</sub>, 298 K) δ 7.94 (s, 2H), 4.28 (t, *J* = 6.7 Hz, 4H), 1.84 – 1.69 (m, 4H), 1.49 – 1.13 (m, 36H), 0.81 (t, 3H). <sup>13</sup>C NMR (100 MHz, CDCl<sub>3</sub>, 298 K) δ 164.40, 136.46, 135.84, 120.05, 66.56, 31.92, 29.64, 29.57, 29.50, 29.35, 29.21, 28.50, 25.96, 22.70, 14.13., HRMS (+APCI) calcd. [M+H<sup>+</sup>]:661.2285 found: 661.2274.



**Scheme S3.** Synthesis of **P2a** via Buchwald-Hartwig reaction.

**P2a:** 2,5-dimethoxybenzene-1,4-diamine (**2a**, 300 mg, 1.78 mmol), didodecyl 2,5-dibromoterephthalate (**3**, 1.175 g, 1.78 mmol), Pd(OAc)<sub>2</sub> (40.0 mg, 0.178 mmol), Xantphos (154.5 mg, 0.267 mmol), and Cs<sub>2</sub>CO<sub>3</sub> (1.739 g, 5.34 mmol) were mixed in toluene (10 mL) in a 50 mL-Schlenk tube. After freeze-pump-thaw for 3 times, the mixture was heated at 130 °C and stirred for 72 h. After cooling down, the mixture was diluted in chloroform and filtered, and then concentrated by the rotatory evaporator. The solid was further purified by Soxhlet washing setup with acetone for 24h. The product **P2a** was obtained as a red powder (0.96 g, 81%). <sup>1</sup>H NMR (400 MHz, CDCl<sub>3</sub>, 298 K) δ 8.75 (s, 2H), 8.01 (s, 2H), 4.23 (t, *J* = 7.0 Hz, 4H), 3.78 (s, 6H), 1.89 – 0.97 (m, 40H), 0.79 (t, *J* = 7.8 Hz, 6H). <sup>13</sup>C NMR (126 MHz, CDCl<sub>3</sub>, 298 K) δ 168.02, 166.29, 159.32, 138.85, 135.42, 130.89, 128.95, 123.50, 118.28, 114.51, 65.44, 32.07, 29.50, 28.75, 26.10, 22.83,

18.19, 17.90, 14.24. FT-IR (ATR) ( $\text{cm}^{-1}$ ): 3356, 2954, 2914, 2848, 1683, 1641, 1535, 1222, 1091, 862, 783. Size exclusion chromatography:  $M_n = 12.6 \text{ kg mol}^{-1}$ ,  $D = 2.02$ .

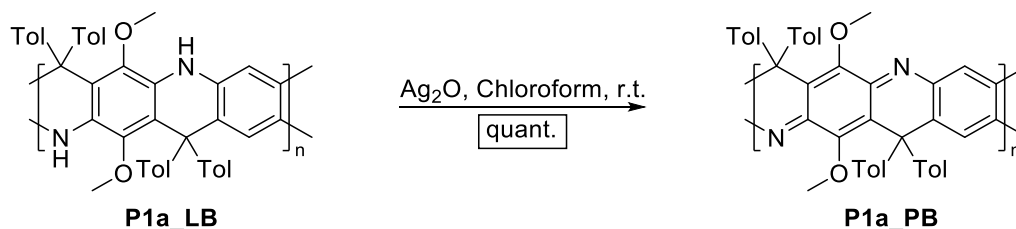


**Scheme S4.** Synthesis of **P1a\_LB** via Grignard reaction and Lewis acid catalyzed ring closure reaction.

**P1a\_LB:** To a solution of *p*-Tol Magnesium Bromide Solution (0.5M in THF, 58 mL), **P2a** solution in THF (50 mL) was added slowly over an ice bath. The reaction was heated to reflux and stirred for 12 h. After cooling to room temperature,  $\text{N}_2\text{H}_4 \cdot \text{H}_2\text{O}$  was added to prevent it oxidizing in air.  $\text{N}_2\text{H}_4\text{Cl}$  (saturated solution) was then added. The mixture was extracted with chloroform. The organic layer was dried over  $\text{MgSO}_4$ . The solution was filtered and dried under vacuum, affording a dark brown solid. The solid was directly used for the next step. To a solution of  $\text{BF}_3 \cdot \text{Et}_2\text{O}$  in  $\text{CH}_2\text{Cl}_2$  (0.5M, 40 mL),  $\text{CH}_2\text{Cl}_2$  solution of the solid obtained from previous step was added slowly while in an ice bath. The reaction was stirred at room temperature for 12 h, and then it was quenched by adding aqueous NaOH solution (1 M). The resulting precipitate was filtered, washed with  $\text{N}_2\text{H}_4 \cdot \text{H}_2\text{O}$  and dried under vacuum. The obtained solid was further purified by Soxhlet washing setup with acetone for 24 h, affording **P1a\_LB** as a brown solid. (0.67 g, 74 %).  $^1\text{H}$  NMR was not able to be obtained because of the easy oxidized nature of **P1a\_LB** in air.  $^{13}\text{C}$  NMR was obtained by adding  $\text{N}_2\text{H}_4 \cdot \text{H}_2\text{O}$  in the sample.  $^{13}\text{C}$  NMR (126 MHz,  $\text{CD}_2\text{Cl}_2$ , 298K)  $\delta$  141.12, 135.68, 132.96, 130.60, 129.94, 129.55, 128.14, 126.44, 119.73, 114.70, 54.96, 20.77. FT-IR

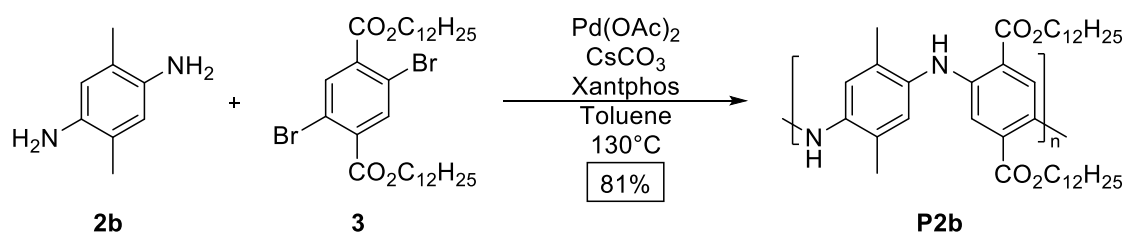
(ATR) ( $\text{cm}^{-1}$ ): 3404, 3097, 2993, 2964, 2829, 1523, 1496, 1465, 1305, 1234, 1099, 804, 781, 717.

Size exclusion chromatography:  $M_n = 11.2 \text{ kg mol}^{-1}$ ,  $\bar{D} = 2.0$ .



**Scheme S5.** Synthesis of **P1a\_PB** via oxidation.

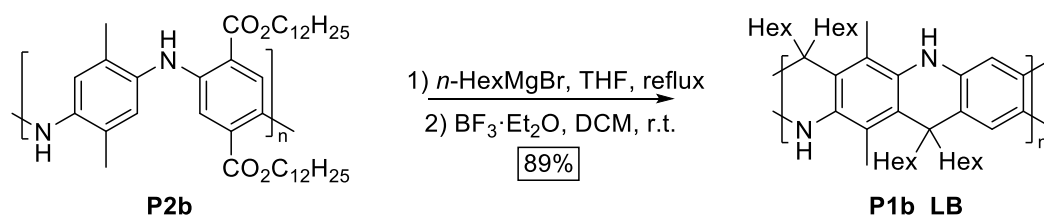
**P1a\_PB:**  $\text{Ag}_2\text{O}$  particle (2 equiv.) was added into a solution of **P1a\_LB** (0.1g) in chloroform (10 mL). The mixture was stirred at room temperature for 12 h. After filtering through filter paper, the solution was dried under vacuum to give the desired compound **P1a\_PB** as a blue solid.  $^1\text{H}$  NMR (400 MHz,  $\text{CD}_2\text{Cl}_2$ , 298 K)  $\delta$  7.20 – 5.68 (m, 18H), 3.03 (s, 6H), 2.28 (s, 12H).  $^{13}\text{C}$  NMR (126 MHz,  $\text{CD}_2\text{Cl}_2$ , 298K)  $\delta$  155.40, 150.49, 147.69, 144.84, 142.43, 137.24, 135.94, 130.73, 129.64, 129.24, 128.45, 55.48, 20.73. FT-IR (ATR) ( $\text{cm}^{-1}$ ): 2951, 2926, 2858, 1608, 1506, 1259, 1074, 1022, 802. Size exclusion chromatography:  $M_n = 11.8 \text{ kg mol}^{-1}$ ,  $\bar{D} = 1.91$ .



**Scheme S6.** Synthesis of **P2b** via Buchwald-Hartwig reaction.

**P2b:** Didodecyl 2,5-dibromoterephthalate (**3**, 1g, 1.52 mmol), 2,5-dimethylbenzene-1,4-diamine (**2b**, 0.207 g, 1.52 mmol),  $\text{Pd(OAc)}_2$  (34.1 mg, 0.152 mmol), Xantphos (131.9 mg, 0.228 mmol), and  $\text{Cs}_2\text{CO}_3$  (1.48 g, 4.56 mmol) were mixed in toluene (10 mL) in a 50 mL-Schlenk tube. After

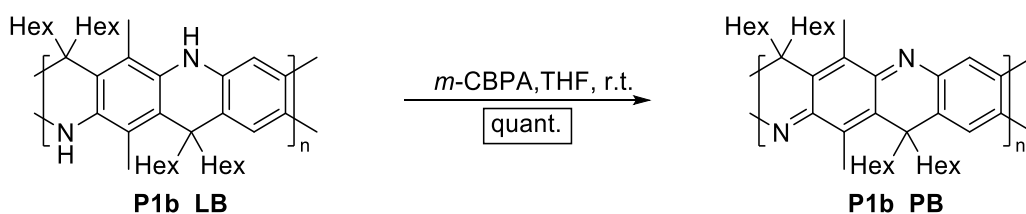
freeze-pump-thaw for 3 times, the mixture was heated at 130°C and stirred for 72 h. After cooling down, the mixture was diluted in chloroform and filtered, and then concentrated by the rotatory evaporator. It was further purified by Soxhlet washing setup with acetone for 24h. The product **P2b** was obtained as a red powder (0.95 g, 79 %). <sup>1</sup>H NMR (500 MHz, CDCl<sub>3</sub>, 298 K) δ 6.90 (s, 2H), 2.85 (s, 6H), 1.39 – 0.97 (m, 52H). <sup>13</sup>C NMR (126 MHz, CDCl<sub>3</sub>, 298 K) δ 167.87, 152.73, 138.69, 132.31, 131.30, 130.63, 128.80, 127.96, 123.35, 118.12, 65.09, 31.92, 29.64, 29.35, 25.95, 22.67, 17.74, 14.09. FT-IR (ATR) (cm<sup>-1</sup>): 3351, 2951, 2909, 2856, 1679, 1524, 1410, 1213, 1088, 771, 694. Size exclusion chromatography: M<sub>n</sub> = 23.2 kg mol<sup>-1</sup>, Đ = 1.95.



**Scheme S7.** Synthesis of **P1b\_LB** via Grignard reaction and Lewis acid catalyzed ring closure reaction.

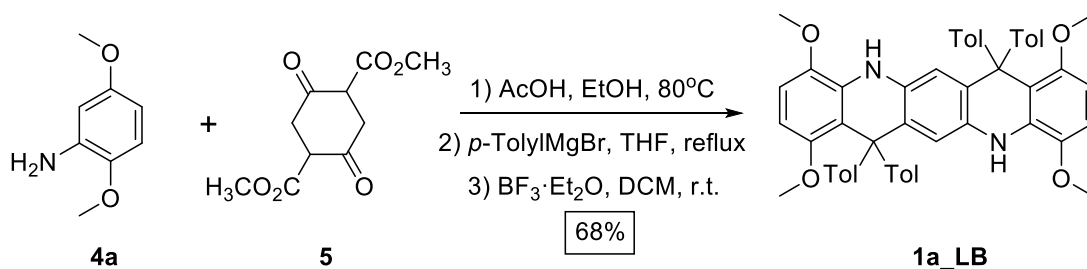
**P1b\_LB:** To a solution of n-Hexylmagnesium Bromide Solution (0.5M in THF, 58 mL), **P2b** solution in THF (50 mL) was added slowly in ice bath. The reaction was heated to reflux and stirred for 12 h. After cooled to room temperature. N<sub>2</sub>H<sub>4</sub>Cl (saturated solution) was added to quench the reaction. The mixture was extracted with chloroform. The organic layer was dried over MgSO<sub>4</sub>. The solution was filtered and dried under vacuum, affording a dark brown solid. The solid was directly used for the next step. To a solution of BF<sub>3</sub>·Et<sub>2</sub>O in CH<sub>2</sub>Cl<sub>2</sub> (0.5M, 40 mL), CH<sub>2</sub>Cl<sub>2</sub> solution of the solid obtained from previous step was added slowly in ice bath. The reaction was stirred at room temperature for 12 h, and was quenched by adding into aqueous NaOH solution (1 M). The resulting precipitate was filtered, washed with N<sub>2</sub>H<sub>4</sub>·H<sub>2</sub>O and dried under vacuum. The

obtained solid was further purified by Soxhlet washing setup with acetone for 24h, affording **P1b\_LB** as a brown solid. (0.88 g, 90 %).  $^1\text{H}$  NMR (500 MHz,  $\text{THF-}d_8$ , 298 K)  $\delta$  6.90 (s, 2H), 2.19 (s, 6H), 1.48 – 0.61 (m, 52H).  $^{13}\text{C}$  NMR (126 MHz,  $\text{THF-}d_8$ , 298K)  $\delta$  152.26, 152.13, 149.60, 146.26, 138.05, 137.95, 135.48, 128.43, 125.40, 34.66, 30.31, 20.91, 13.99. FT-IR (ATR) ( $\text{cm}^{-1}$ ):3436, 2958, 2922, 2854, 1514, 1463, 1388, 1219, 1112, 995, 871, 725. Size exclusion chromatography:  $M_n = 20.3 \text{ kg mol}^{-1}$ ,  $\text{Đ} = 1.73$ .



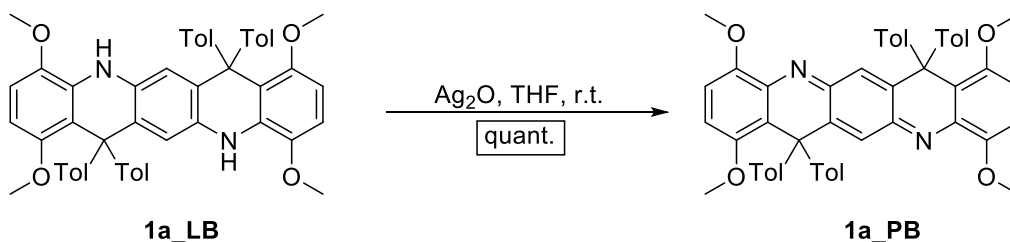
**Scheme S8.** Synthesis of **P1b\_PB** via oxidation.

**P1b\_PB:** Meta-chloroperoxybenzoic acid (*m*-CPBA) (2 equiv.) was added into a solution of **P1b\_LB** (0.1g) in chloroform (10 mL). The mixture was stirred at room temperature for 12 h. The reaction was poured into NaOH (1M) solution and extracted with chloroform. The organic phase was dried over  $\text{Na}_2\text{SO}_4$  and filtered. The solvent was evaporated under vacuum to obtain blue powder **P1b\_PB**.  $^1\text{H}$  NMR (500 MHz,  $\text{THF-}d_8$ , 298K)  $\delta$  6.58 (s, 2H), 2.54 (s, 6H), 1.31 – 0.77 (m, 52H).  $^{13}\text{C}$  NMR (126 MHz,  $\text{THF-}d_8$ , 298K)  $\delta$  186.26, 145.80, 144.28, 134.72, 133.11, 131.13, 130.42, 129.58, 129.13, 128.34, 128.07, 70.87, 39.50, 34.60, 32.40, 29.38, 13.95, 10.88. FT-IR (ATR) ( $\text{cm}^{-1}$ ):2922, 2848, 2794, 1645, 1452, 1363, 1257, 1095, 806. Size exclusion chromatography:  $M_n = 21.2 \text{ kg mol}^{-1}$ ,  $\text{Đ} = 1.76$ .



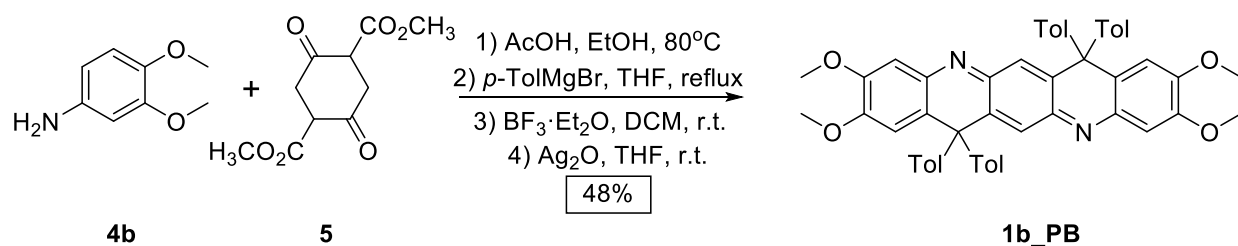
**Scheme S9.** Synthesis of **1a\_LB** via imine condensation, followed by Grignard reaction and Lewis acid catalyzed ring closure reaction.

**1a\_LB:** **4a** (1.0 g, 6.54 mmol), **5** (0.6 g, 2.6 mmol), EtOH (50 mL) and acetic acid (10 mL) were mixed in a round bottom flask and heated to reflux overnight. After cooling to room temperature, the solid was washed with MeOH. The pink solid obtained was dried under vacuum and directly used for next step. To a solution of *p*-Tolylmagnesium bromide (20 mL, 0.5 M in THF) under nitrogen protection, the solid from the previous step solution in THF (5 mL) was added dropwise. The reaction was heated to reflux for 12 h. After cooling to room temperature, the mixture was poured into saturated  $\text{NH}_4\text{Cl}$  aqueous solution, and extracted with ethyl acetate. The organic layer was dried with  $\text{MgSO}_4$  and filtered. After removing solvent by rotatory evaporator, the crude product was dissolved in  $\text{CH}_2\text{Cl}_2$  (10 mL).  $\text{BF}_3 \cdot \text{Et}_2\text{O}$  (1 mL, 0.3 M) was added into the solution and the reaction was stirred at room temperature for 12 h under nitrogen protection. The reaction was quenched with NaOH aqueous solution (1 M) and extracted with  $\text{CH}_2\text{Cl}_2$ . The organic layer was dried over  $\text{MgSO}_4$  and purified with flash column chromatography (silica, hexane). The pure **1a\_LB** was collected as a white solid (1.4 g, 68%).  $^1\text{H}$  NMR (500 MHz,  $\text{CD}_2\text{Cl}_2$ , 298K)  $\delta$  7.02 (s, 17H), 6.69 (d,  $J = 8.5$  Hz, 2H), 6.58 (s, 2H), 6.29 (d,  $J = 8.5$  Hz, 2H), 6.15 (s, 2H), 3.79 (s, 6H), 3.16 (s, 6H), 2.30 (s, 12H).  $^{13}\text{C}$  NMR (126 MHz,  $\text{CD}_2\text{Cl}_2$ , 298K)  $\delta$  152.71, 145.17, 140.35, 135.07, 132.42, 130.84, 129.31, 128.09, 116.45, 115.98, 108.40, 102.95, 55.96, 55.59, 20.73. HRMS (+APCI) calcd.  $[\text{M}+\text{H}]^+$ : 765.3687 found: 765.3651.



**Scheme S10.** Synthesis of **1a\_PB** via Oxidation of **1a\_LB**.

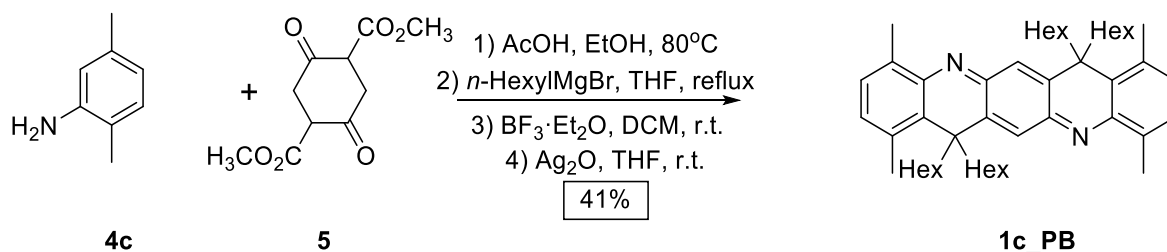
**1a\_PB:** Ag<sub>2</sub>O particle (2 equiv.) was added into a solution of **1a\_LB** (1g) in THF (10 mL). The mixture was stirred at room temperature for 12 h. After filtering through filter paper, the solution was dried under vacuum to give the desired compound **1a\_PB** as a deep-red solid (0.98g, quant.). <sup>1</sup>H NMR (500 MHz, CD<sub>2</sub>Cl<sub>2</sub>, 298K) δ 7.04 (s, 16H), 6.88 (d, *J* = 9.1 Hz, 2H), 6.81 (d, *J* = 9.1 Hz, 2H), 6.55 (s, 2H), 3.87 (s, 6H), 3.13 (s, 6H), 2.31 (s, 12H). <sup>13</sup>C NMR (101 MHz, CD<sub>2</sub>Cl<sub>2</sub>, 298K) δ 153.40, 151.88, 143.15, 142.77, 136.48, 136.08, 135.36, 134.82, 129.41, 129.03, 128.69, 125.25, 115.50, 111.22, 56.50, 56.17, 21.02. HRMS (+APCI) calcd. [M+H<sup>+</sup>]:763.3530 found: 763.3492.



**Scheme S11.** Synthesis of **1b\_PB** via imine condensation, followed by Grignard reaction, Lewis acid catalyzed ring closure reaction and oxidation.

**1b\_PB:** **1b\_PB** was synthesized as synthetic route of **1a\_PB** through **4b** and **5**. <sup>1</sup>H NMR (500 MHz, CD<sub>2</sub>Cl<sub>2</sub>, 298K) δ 6.99 (d, *J* = 8.1 Hz, 8H), 6.91 (s, 2H), 6.85 (d, *J* = 8.3 Hz, 8H), 6.50 (s, 2H), 6.39 (s, 2H), 3.75 (s, 6H), 3.55 (s, 6H), 2.24 (s, 12H). <sup>13</sup>C NMR (101 MHz, CD<sub>2</sub>Cl<sub>2</sub>, 298K) δ

153.03, 149.06, 148.69, 141.65, 138.93, 136.83, 135.38, 129.70, 128.78, 128.67, 113.12, 112.42, 56.80, 55.94, 20.63. HRMS (+APCI) calcd. [M+H<sup>+</sup>]:763.3530 found: 763.3517.



**Scheme S12.** Synthesis of **1c\_PB** via imine condensation, followed by Grignard reaction, Lewis acid catalyzed ring closure reaction and oxidation.

**1c\_PB:** **1c\_PB** was synthesized as synthetic route of **1a\_PB** through **4c**, **5** and *n*-HexylMgBr. <sup>1</sup>H NMR (500 MHz, THF-*d*<sub>8</sub>, 298K) δ 7.02 (s, 2H), 6.96 (d, *J* = 7.7 Hz, 2H), 6.83 (d, *J* = 7.7 Hz, 2H), 2.45 (s, 6H), 2.41 (s, 6H), 1.11 – 0.61 (m, 52H). <sup>13</sup>C NMR (126 MHz, THF-*d*<sub>8</sub>, 298K) δ 175.25, 153.92, 144.71, 141.52, 136.65, 133.05, 132.87, 130.72, 128.76, 46.77, 43.71, 31.51, 29.56, 22.39, 18.13, 13.32. HRMS (+APCI) calcd. [M+H<sup>+</sup>]:675.5612 found: 675.5605.

### 3. Oxidation, Reduction, and Protonation Titration

The chemical oxidation of LLB to LPB was monitored with UV-vis spectroscopy (**Figure S1a**) when a *m*-CPBA solution was added from 0 to 1.0 equivalent into a solution of **P1a\_LB** in THF (concentration of repeating units = 1 mM). The initial **P1a\_LB** solution was already partially oxidized by air because of the electron rich nature of **P1a\_LB**. The peak centered at 650 nm increased as a result of the further generation of conjugated cyclohexadiene-1,4-diimine unit moieties. A clear isosbestic point indicated a well-defined transformation from **P1a\_LB** to **P1a\_PB**. UV-Vis spectroscopy were also recorded when an increasing amount of diethylhydroxylamine (DEHA) was added from 0 to 2.0 equivalent into a solution of **P1a\_PB** in

THF (concentration of repeating units = 1 mM). The peak at 650 nm disappeared because of the reduction of the cyclohexadiene-1,4-diimine unit moieties in **PB** state, to the benzene-diamine unit in **LB** state. Clear isosbestic point indicated a reversible transformation from **P2a\_PB** to **P2a\_LB** (**Figure S1b**).

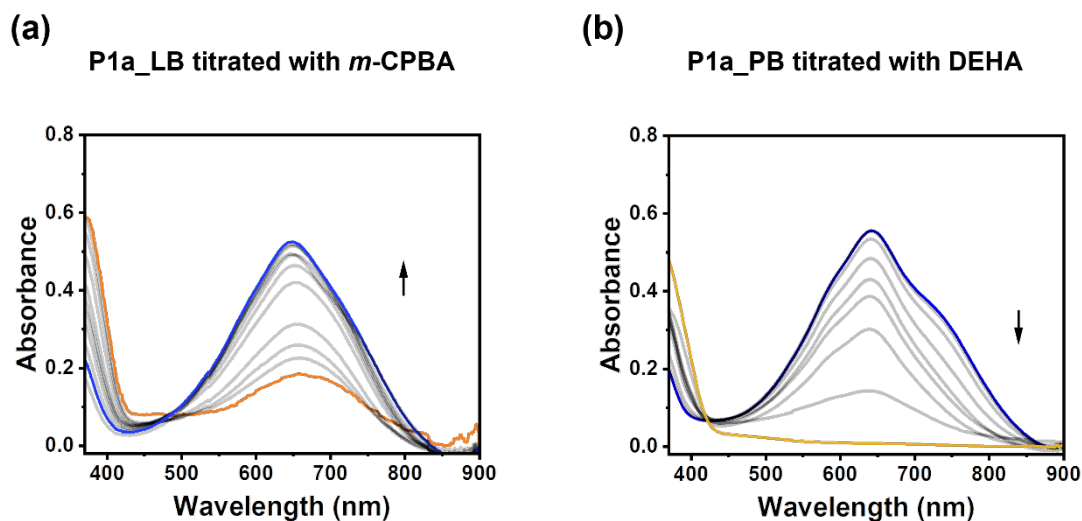


**Figure S1.** (a) Oxidation of **P1a\_LB** to **P1a\_PB**. (b) Reduction of **P1a\_PB** to **P1a\_LB**.

Protonation experiments were performed for **P1a\_PB**, **1a\_PB**, **P1b\_PB**, **1c\_PB** and monitored using UV-vis spectroscopy. The titration process for **1a\_PB** and **1c\_PB** was followed as: a solution of Methanesulfonic acid (MSA) in THF ( $5 \text{ mol L}^{-1}$ , 0-200  $\mu\text{L}$ ) was added into **1a\_PB** (**Figure S2a**, top) or **1c\_PB** (**Figure S2b**, bottom) solution (2.5 mL,  $1 \times 10^{-5} \text{ mol L}^{-1}$ ). The titration of **1a\_PB** showed a two-stage process: firstly, the disappearance of peak centered 350 nm and generation of the peak centered at 550 nm, and then secondly, disappearance of the peak centered at 550 nm and an appearance of a broad peak centered at 800 nm, corresponding to the binding of two protons for each molecule. As a contrast, the titration of **1c\_PB** only had the first stage, and even though more MSA was added, the peak centered at around 550 nm didn't decrease. The fitting of the binding constant between molecules and protons and calculation of mole fractions data fitting was

independently corroborated using an online fitting tool Bindfit.<sup>3, 4</sup> The models selected were UV 1:2 for **1a\_PB**, corresponding to the two stage of protonation, and UV 1:1 for **1c\_PB**, which means each of the molecule only could react with one proton during the process. The input files were lists of concentrations of MSA and **1a\_PB** or **1c\_PB**.

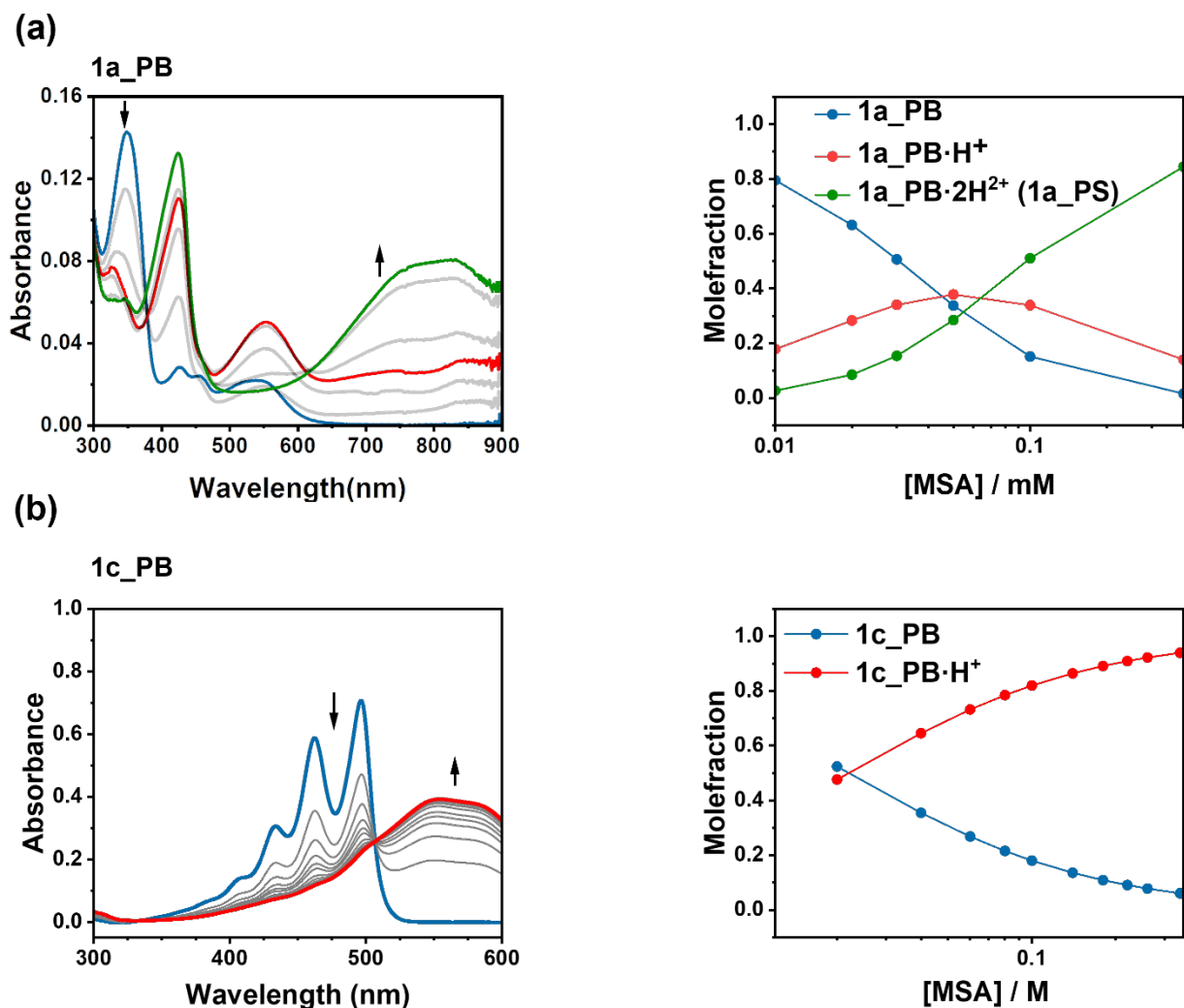


**Figure S2.** UV-vis-NIR absorption spectra (left) and mol-fraction calculated using Bind-fit (right) corresponding to doping process of (a) **1a\_PB** and (b) **1c\_PB** with increasing amount of MSA.

The fitting output binding constant of **1a\_PB** with H<sup>+</sup> to be  $K_1 \approx 44 \text{ M}^{-1}$  and  $K_2 \approx 30 \text{ M}^{-1}$ , and **1c\_PB** with H<sup>+</sup> to be  $K_1 \approx 45 \text{ M}^{-1}$ .

#### 4. Conductivity Optimization

In this study, we investigated a two-dimensional experimental space comprising of the following parameters: acid type and equivalents. A total of 12 distinct types of acids and 10 different levels of equivalents (ranging from 1 to 10) were treated as categorical variables. To facilitate the exploration of this experimental space, we employed the SUMMIT code<sup>5</sup> to define the search domain and applied the Latin Hypercube Sampling (LHS) approach<sup>6</sup> to suggest the experimental conditions for exploration.

The acid species and equivalent to dope **P1a\_PB** for conductivity test of this polymer were screened using the autonomous Polybot system at the Argonne National Laboratory. The formula was first optimized based on different acid species and fixed thickness (~20nm, by fixing the concentration of **P1a\_PB** to be 1 mg mL<sup>-1</sup> in THF, and rate of spin coating as 2000rpm for 30s). The data obtained from the exploratory cycles are listed in the **Table S1**:

**Table S1.** High-throughput data of **P1a\_PB**

Acid	Ratio	Conductivity (S cm <sup>-1</sup> )
CuCl <sub>2</sub>	7	0.00189
CuCl <sub>2</sub>	7	2.78×10 <sup>-4</sup>
FeCl <sub>3</sub>	2	5.26×10 <sup>-7</sup>
FeCl <sub>3</sub>	9	0.00088
FeCl <sub>3</sub>	10	0.00097

FeCl <sub>3</sub>	7	0.00046
HBr	2	0.00021
HBr	1	2.33×10 <sup>-4</sup>
<b>HBr</b>	<b>10</b>	<b>0.00455</b>
<b>HBr</b>	<b>8</b>	<b>0.00117</b>
<b>HBr</b>	<b>7</b>	<b>0.00149</b>
<b>HCl</b>	<b>10</b>	<b>0.00749</b>
<b>HCl</b>	<b>6</b>	<b>0.00559</b>
<b>HCl</b>	<b>4</b>	<b>0.00323</b>
<b>HCl</b>	<b>7</b>	<b>0.00535</b>
HOAc	1	1.67×10 <sup>-6</sup>
HOAc	1	7.69×10 <sup>-7</sup>
HOAc	3	0.00044
HOAc	7	0.00036
LiBF <sub>4</sub>	8	0.00075
LiBF <sub>4</sub>	7	0.00048
LiBF <sub>4</sub>	4	0.00083

<b>LiClO<sub>4</sub></b>	<b>8</b>	<b>0.00194</b>
LiClO <sub>4</sub>	8	0.00056
LiClO <sub>4</sub>	10	0.00077
LiClO <sub>4</sub>	8	0.00083
LiClO <sub>4</sub>	1	0.00061
MSA	4	$1.67 \times 10^{-6}$
MSA	2	$1.37 \times 10^{-6}$
MSA	7	0.00067
MSA	1	0.00033
<b>MSA</b>	<b>9</b>	<b>0.00126</b>
MSA	10	0.00051
NiCl <sub>2</sub>	1	$1.43 \times 10^{-6}$
NiCl <sub>2</sub>	2	$1.47 \times 10^{-7}$
NiCl <sub>2</sub>	2	$1.54 \times 10^{-6}$
NiCl <sub>2</sub>	2	$1.75 \times 10^{-6}$
NiCl <sub>2</sub>	6	$4.42 \times 10^{-5}$
<b>NiCl<sub>2</sub></b>	<b>9</b>	<b>0.00102</b>

NiCl <sub>2</sub>	4	0.00042
PTSA	3	0.00071
TFA	5	0.00056
TFA	3	0.00056
<b>ZnCl<sub>2</sub></b>	<b>5</b>	<b>0.00122</b>
ZnCl <sub>2</sub>	3	1.67×10 <sup>-7</sup>
ZnCl <sub>2</sub>	2	6.25×10 <sup>-7</sup>
ZnCl <sub>2</sub>	5	0.00052
ZnCl <sub>2</sub>	10	0.00048

## 5. Paramagnetism Characterization

Electron paramagnetic resonance (EPR) spectrometry was conducted on a Bruker ELEXSYS II E500 with microwave frequency of ca. 9.38 GHz at 288 K. A 4 mm ID sample tube was used for solids samples. The spectra were acquired at 1 G modulation and 100 kHz modulation frequency. The *x*-axis represents the *g* factor, and the *y*-axis represents the intensity per mole of repeating unit. The *g* factors were calculated based on the following equation in which *ν* is the microwave frequency and *B* is the resonance magnetic field:

$$g = \frac{71.4484 \times \nu \text{ (GHz)}}{B \text{ (mT)}}$$

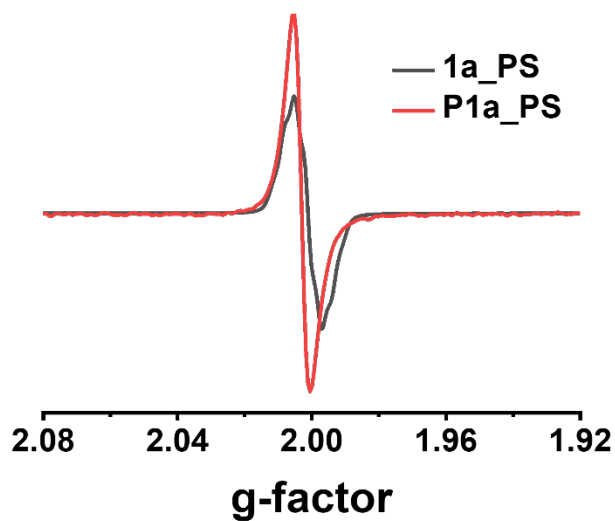


**Figure S3.** EPR spectra of **1a\_PS** and **P1a\_PS** solids (**1a\_PB** and **P1a\_PS** doped with 2 equivalents of PTSA).

Magnetic measurements were conducted on a Quantum Design MPMS XL SQUID magnetometer from 2 to 300K under an external magnetic field of 1000 Oe. The magnetization measurements were performed at 2 K over the magnetic field range of 250-70000 Oe. The diamagnetic contributions of the sample holders and the atoms were corrected with blank holders and the Pascal's constants. **1a\_PB**, **1c\_PB**, **P1a\_PB** and **P1b\_PB** were mixed with 4 equivalents of *p*-Toluenesulfonic acid (PTSA) and dried under vacuum to remove water, and the obtained powder was measured. Acid mixed **1c\_PB** and **P1b\_PB** did not exhibit dominant temperature-independent

paramagnetism (**Figure S3**), which was attributed to their lack of basicity.

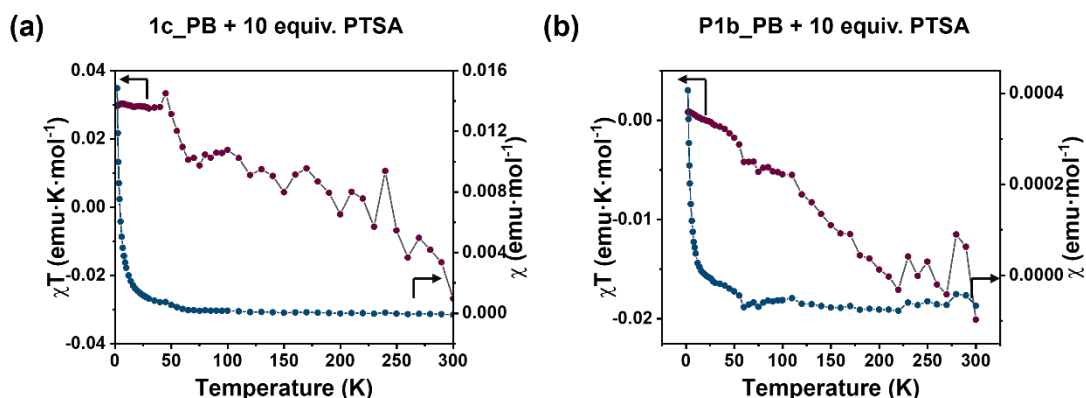


**Figure S4.** Temperature-varied magnetic susceptibility of 10 equivalents PTSA mixed (a) **1c\_PB** and (b) **P1b\_PB**.

Magnetic measurements were also performed at 2 K to investigate the spin ground states of these pernigraniline salt analogues (**Figure S4**). The magnetization data for protonated **1a\_PB** (**1a\_PS**) and **P1a\_PB** (**P1a\_PS**) are in accord with a triplet ground state ( $S = 1$ ) with a small positive coupling constant ( $0.12 \text{ cm}^{-1}$  and  $0.5 \text{ cm}^{-1}$ ), suggesting a weak ferromagnetic coupling between the radical pair. Such coupling is likely facilitated by the rigidity and coplanarity of the conjugated ladder-type backbone.

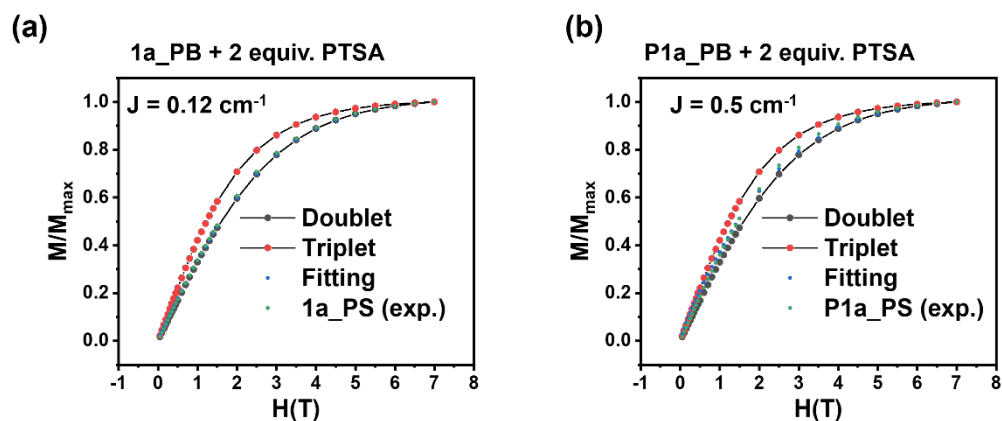


**Figure S5.** Field-varied magnetic susceptibility of 2 equivalents PTSA mixed (a) **1a\_PS** (**1a\_PB** + 2 equiv. PTSA) and (b) **P1a\_PS** (**P1a\_PB** + 2 equiv. PTSA).

## 6. Diradical Character Calculation

**1b\_PS** was calculated based on the single crystal structure without optimization. The occupancy number of highest occupied natural orbital ( $\sigma_{\text{HONO}}$ ) and lowest unoccupied natural orbital ( $\sigma_{\text{LUNO}}$ ), and corresponding diradical character  $y$  were calculated at UHF/6-31+G(d,p) level of theory.

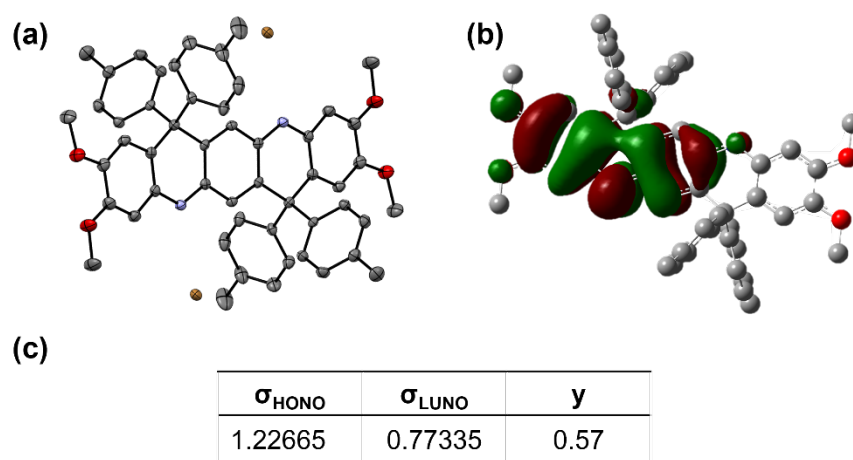


**Figure S6.** (a) Single crystal of **1c\_PS**<sup>2+</sup>·2Br<sup>-</sup> (**1c\_PS**); (b) spin density distribution of **1c\_PS**; (c) Calculated diradical character of **1c\_PS**.

## 7. Cyclic voltammetry and Spectroelectrochemistry

Cyclic voltammetry (CV) was performed in a three-electrode system with Ag/AgCl as the reference electrode and a platinum wire as the counter electrode. Ferrocene/Ferrocene<sup>+</sup> (Fc/Fc<sup>+</sup>) was used as the external reference. TBAPF<sub>6</sub> solution in THF (0.1 mol L<sup>-1</sup>), MSA in THF (0.15 mol L<sup>-1</sup> for **1a** and **P1a**, 1 mol L<sup>-1</sup> for **1c** and **P1b**, for the purpose of effective protonation) and LiClO<sub>4</sub> solution in THF (1.0 mol L<sup>-1</sup>) were used as the electrolyte depending on the experimental setting. For solution-phase measurement, a 3 mm glass-carbon electrode was used as the working electrode. For thin-film measurement, a piece of ITO-coated glass with spin-coated polymer thin film was used as the working electrodes. **P1a**\_PB sample was spin-coated on the ITO-coated glass as a thin film from its THF solutions (10 mg mL<sup>-1</sup>, 2000 rpm for 120 s) and annealed at 100 °C for 10 min in a glovebox. The scan rate was set as 100 mV s<sup>-1</sup>.

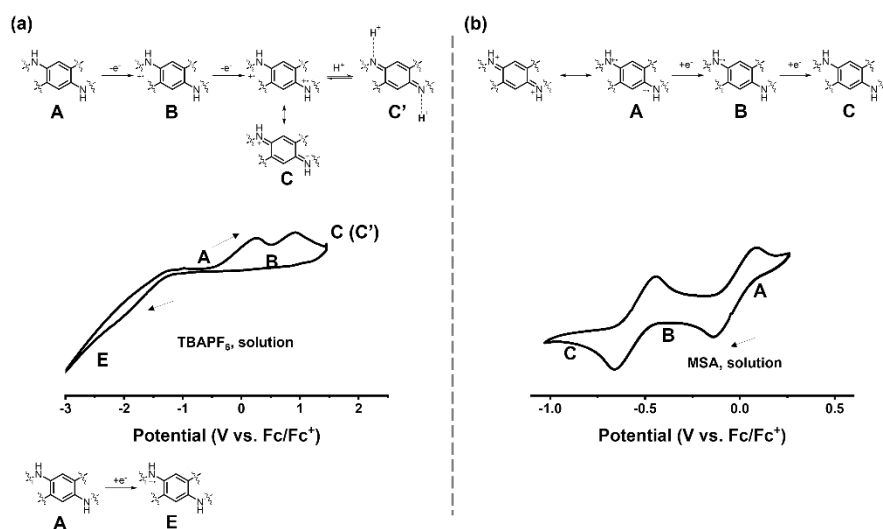


**Figure S7.** Cyclic voltammograms of (a) **1a**\_LB solution in THF with 0.1 mol L<sup>-1</sup> TBAPF<sub>6</sub>. (b) **1a**\_PB solution in THF with 0.15 mol L<sup>-1</sup> MSA.

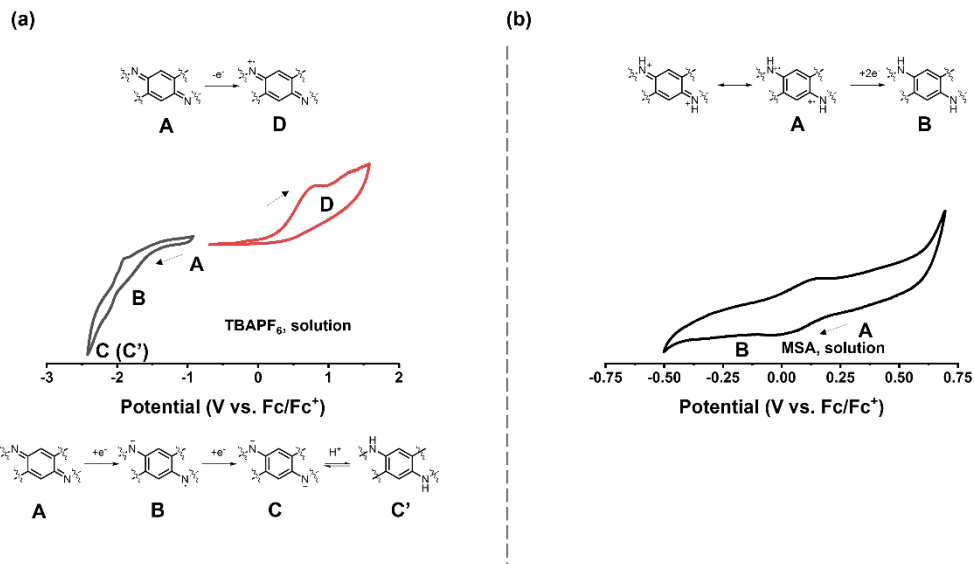


**Figure S8.** Cyclic voltammograms of (a) **P1a\_PB** solution in THF with 0.1 mol L<sup>-1</sup> TBAPF<sub>6</sub>. (b) **P1a\_PB** solution in THF with 0.15 mol L<sup>-1</sup> MSA.

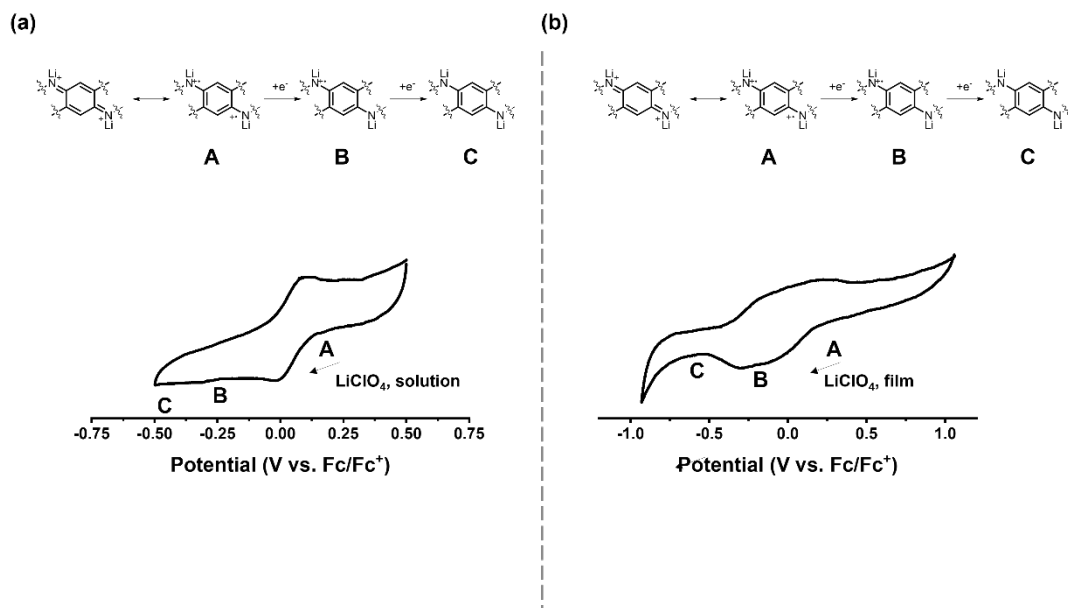


**Figure S9.** Cyclic voltammograms of **P1a\_PB** solution in THF with 1.0 mol L<sup>-1</sup> LiClO<sub>4</sub>. (b) **P1a\_PB** film in acetonitrile with 1.0 mol L<sup>-1</sup> LiClO<sub>4</sub>.

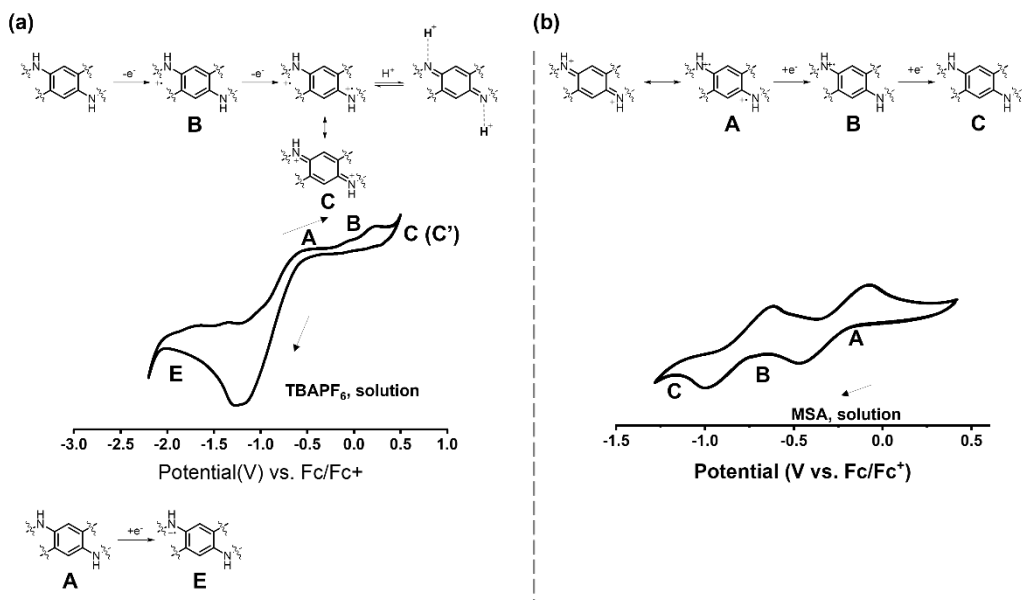


**Figure S10.** Cyclic voltammograms of (a) **1b<sub>LB</sub>** solution in THF with 0.1 mol L<sup>-1</sup> TBAPF<sub>6</sub>. (b) **1b<sub>PB</sub>** solution in THF with 1 mol L<sup>-1</sup> MSA.

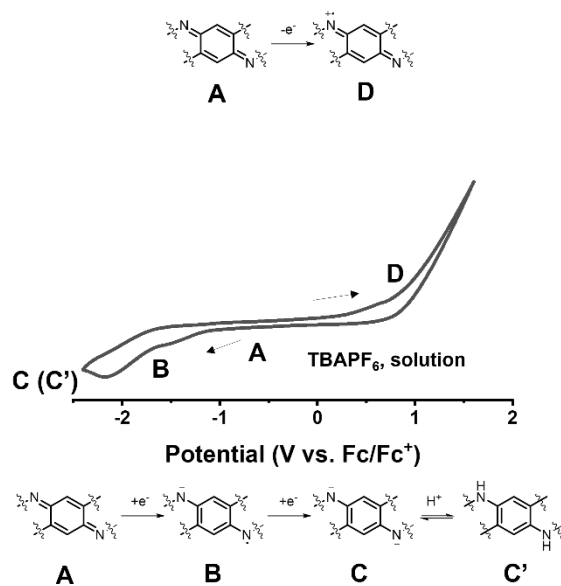


**Figure S11.** Cyclic voltammograms of (a) **P1b<sub>PB</sub>** solution in THF with 0.1 mol L<sup>-1</sup> TBAPF<sub>6</sub>.

## 8. Stability Measurement in 99% MSA.

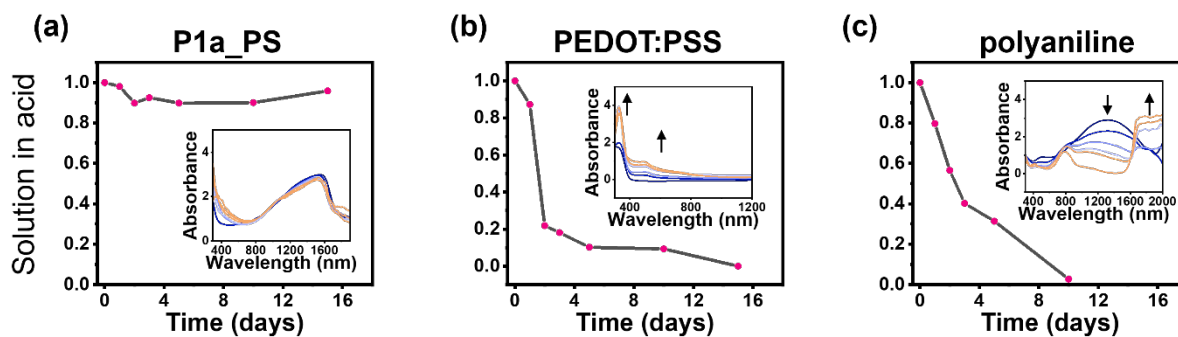


**Figure S12.**  $1\text{ mg mL}^{-1}$  of (a) **P1a\_PB** (becomes **P1a\_PS** in MSA solution), (b) PEDOT:PSS (middle), and (c) polyaniline in 99% MSA solution.

## 9. Electrochemical Stability Measurement

**P1a\_PB** was employed as the active material in a sandwiched electrochromic device, which was fabricated with two ITO–glass substrates, a spin-cast **P1a\_PB** thin film, and lithium gel electrolyte (PMMA/PC/LiClO<sub>4</sub>). When 2.0 V voltage was applied on the **P1a\_PB** layer, the device showed a pale-yellow color with an absorption peak at around 350 nm, corresponding to the **P1a\_LB** state. As the voltage switched to +2.0 V, the device turned a deep blue color and a broad absorption peak evolved in the NIR region ( $\lambda_{\text{max}} = 900\text{ nm}$ ), corresponding to the lithiated **P1a\_PS** state. The color-switching cyclability was studied by applying alternating working voltage at  $-2.0\text{ V}$  and  $+2.0\text{ V}$  for 30 s at each stage, leading to fully reversible transitions of the absorption between the LB and PS states, in agreement with the solid-state CV results. Only less than 2% decay was observed for the absorption at 900 nm after 200 cycles.

The same device was fabricated with PEDOT:PSS and the same voltage window was applied. The absorbance was recorded at 600 nm. It showed obvious decay (75%) after 50 cycles.

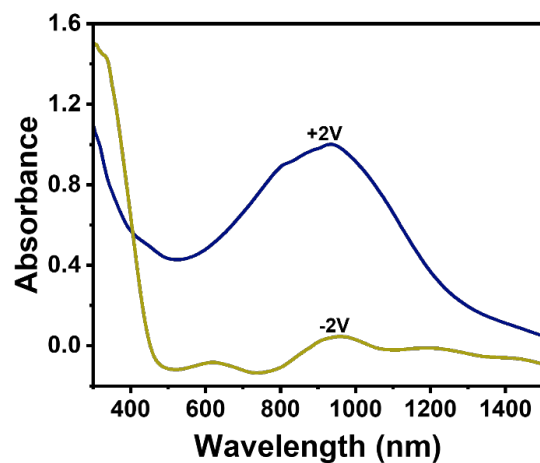
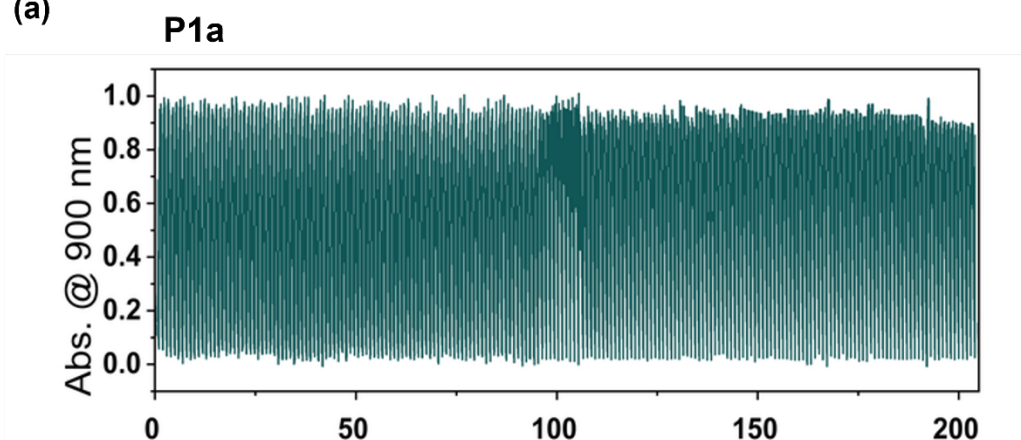
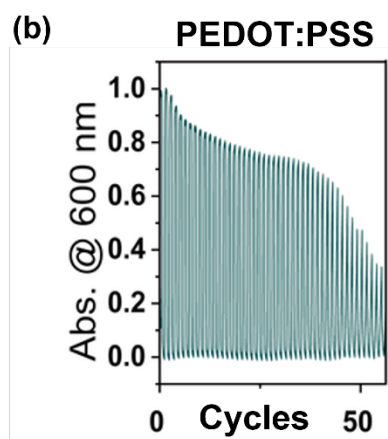


**Figure S13.** Absorption spectra of **P1a\_PB** the electrochromic device when applying  $-2.0$  V (yellow) or  $+2.0$  V (blue) for 60 s.

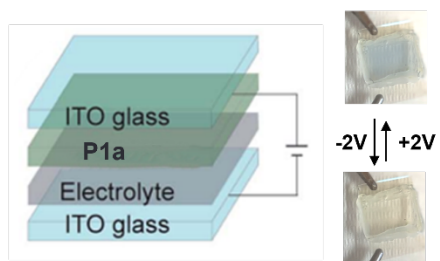
(a)



(b)



(c) **Cycles**



**Electrolyte:  $\text{LiClO}_4/\text{PC}/\text{PMMA}$**

**Figure S14.** (a) Absorbance at 900 nm of electrochromic device, with **P1a** as active material, with voltage swept between  $-2.0$  V and  $+2.0$  V for 200 cycles (120s for one cycle). (b) Absorbance at 900 nm of electrochromic device, with PEDOT:PSS as active material, with voltage swept between  $-2.0$  V and  $+2.0$  V for 60 cycles (120s for one cycle). (c) Architecture and photographic images of the electrochromic device at 2.0 V and  $+2.0$  V, respectively.

### 10. Galvanostatic charge-discharge curves (GCD) of Supercapacitor setup

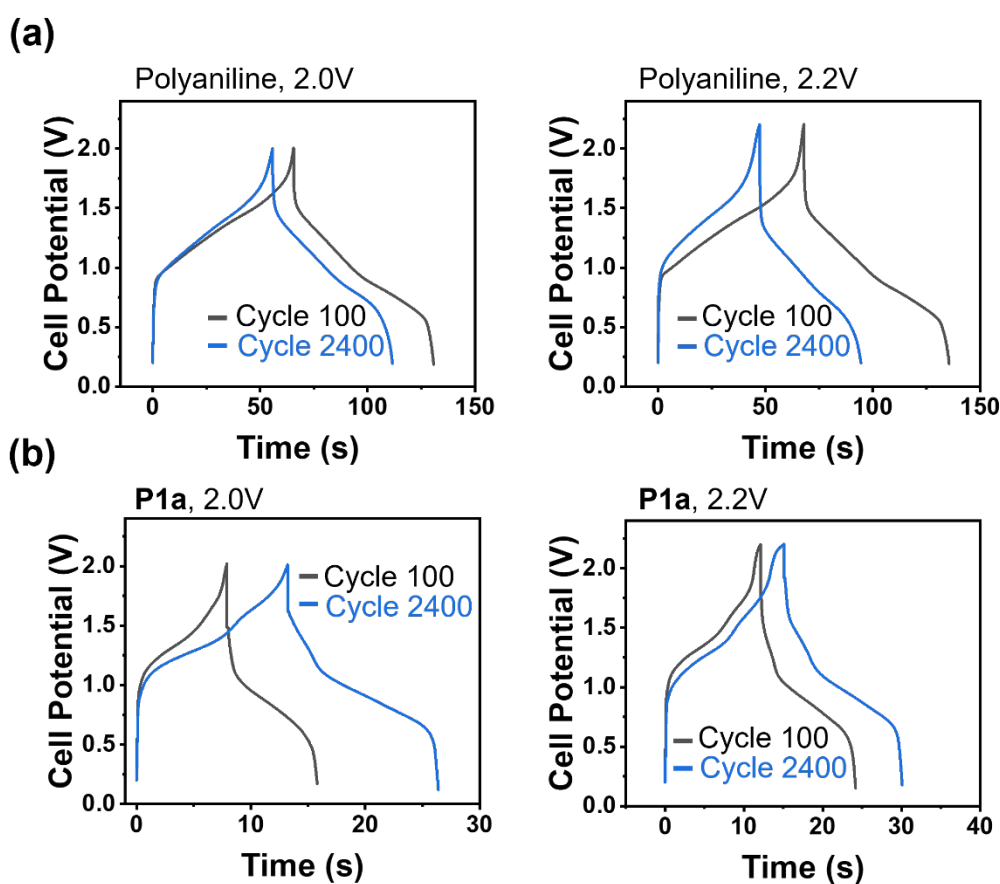


**Figure S15.** Corresponding galvanostatic charge-discharge curves (GCD) of (a) polyaniline and (b) **P1a** at the start and end of cycling.

### 11. Thermogravimetric Analysis (TGA)

TGA was undertaken with a TA Q500 thermogravimetric analyzer in nitrogen flow at 60.0 mL min<sup>-1</sup> at a heating rate of 10.00 °C min<sup>-1</sup>. Both **1a\_PB** and **P1a\_PB** showed around 40% residue weight at 900 °C. The weight loss began at around 150°C was attributed to the cleavage of tolyl side chain (57 wt%) and the conversion of sp<sup>3</sup> carbon into more thermodynamically favorable sp<sup>2</sup> carbon. The weight loss around 230500°C was attributed to the cleavage of methoxy side chains (~10 wt%). **P1a\_LB** was thermally more stable than **P1a\_PB**, but because it's partially oxidized in air, it also exhibited the weight loss beginning at around 150°C.

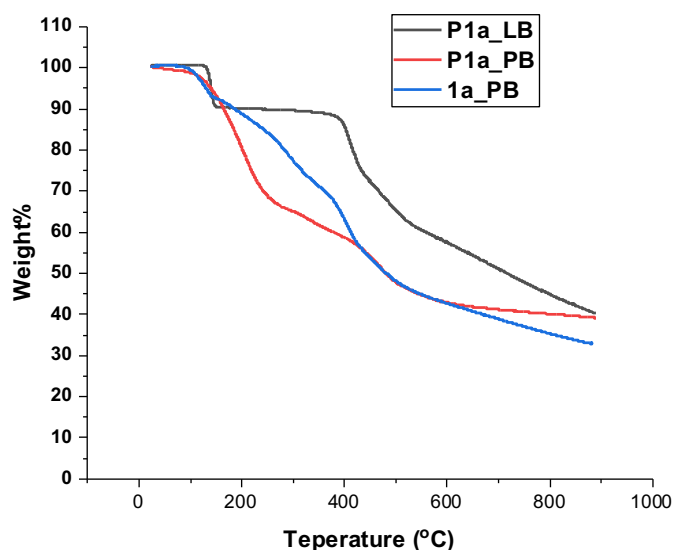


**Figure S16.** TGA plots of **P1a** and **1a** in nitrogen.

## 12. X-ray Crystallography

A Leica MZ 75 microscope was used to identify a representative sample of crystals of the same habit. The crystal was mounted on a nylon loop was then placed in a cold nitrogen stream (Oxford) maintained at 100 K. A BRUKER Venture X-ray (kappa geometry) diffractometer was employed for crystal screening, unit cell determination, and data collection. The goniometer was controlled

using the APEX3 software suite. The sample was optically centered with the aid of a video camera such that no translations were observed as the crystal was rotated through all positions. The X-ray radiation employed was generated from a Cu- $\mu$ s X-ray tube ( $K\alpha = 1.5418\text{\AA}$  with a potential of 50 kV and a current of 1.0mA). 45 data frames were taken at widths of  $1^\circ$ . These reflections were used to determine the unit cell. The unit cell was verified by examination of the h k l overlays on several frames of data. No super-cell or erroneous reflections were observed. After careful examination of the unit cell, an extended data collection procedure (30 sets) was initiated using omega and phi scans. Integrated intensity information for each reflection was obtained by reduction of the data frames with the program APEX3. The integration method employed a three-dimensional profiling algorithm and all data were corrected for Lorentz and polarization factors, as well as for crystal decay effects. Finally, the data was merged and scaled to produce a suitable data set. The absorption correction program SADABS was employed to correct the data for absorption effects. A solution was obtained readily ( $Z=1$ ;  $Z'=0.5$ ) using XT/XS in APEX3. Hydrogen atoms were placed in idealized positions and were set riding on the respective parent atoms. All non-hydrogen atoms were refined with anisotropic thermal parameters. Appropriate restraints and constraints were used to keep the bond distances, angles and thermal ellipsoids meaningful. Absence of additional symmetry or void were confirmed using PLATON (ADDSYM). The structure was refined (weighted least squares refinement on  $F^2$ ) to convergence. Olex2 was employed for the final data presentation and structure plots.

**Table S2.** Crystal data and structure refinement for **1a\_LB**

<b>Bond precision:</b>	C-C = 0.0022 $\text{\AA}$	Wavelength=1.54178	
<b>Cell:</b>	a=10.1190 (4) $\text{\AA}$	b=13.7179(5) $\text{\AA}$	c=15.1622(6) $\text{\AA}$

	alpha=80.631(2) °	beta=77.512(2) °	gamma=74.361(2) °
<b>Temperature:</b>	110 K		
	<b>Calculated</b>	<b>Reported</b>	
<b>Volume</b>	1966.56 (13) Å <sup>3</sup>	1966.56 (13) Å <sup>3</sup>	
<b>Space group</b>	P -1	P -1	
<b>Hall group</b>	-P 1	-P 1	
<b>Molecular formula</b>	C <sub>52</sub> H <sub>48</sub> N <sub>2</sub> O <sub>4</sub>	C <sub>52</sub> H <sub>48</sub> N <sub>2</sub> O <sub>4</sub>	
<b>Sum formula</b>	C <sub>52</sub> H <sub>48</sub> N <sub>2</sub> O <sub>4</sub>	C <sub>52</sub> H <sub>48</sub> N <sub>2</sub> O <sub>4</sub>	
<b>Mr</b>	764.92	764.92	
<b>Density, g cm<sup>-3</sup></b>	1.292	1.292	
<b>Z</b>	2	2	
<b>Mu (mm<sup>-1</sup>)</b>	0.637	0.637	
<b>F000</b>	812	812	
<b>F000'</b>	814.29		
<b>h,k,lmax</b>	12,16,18	12,16,18	
<b>Nref</b>	7503	7459	
<b>T<sub>min</sub>,T<sub>max</sub></b>	0.927,0.958	0.488,0.586	
<b>T<sub>min</sub>'</b>	0.927		

Correction method= # Reported T Limits: T<sub>min</sub>=0.488 T<sub>max</sub>=0.586

AbsCorr = MULTI-SCAN

Data completeness= 0.994

Theta(max)= 70.267

R(reflections)= 0.0489 (6063)

wR2(reflections)= 0.1431 (7459)

S = 1.035

Npar= 582

**Table S3.** Crystal data and structure refinement for **1c\_PB**

<b>Bond precision:</b>	C-C = 0.0017 Å	Wavelength=0.71073	
<b>Cell:</b>	a= 24.6382 (14) Å	b=10.7607 (6) Å	c= 18.6232 (18) Å
	alpha=90 °	beta= 124.745 (1) °	gamma=90 °
<b>Temperature:</b>	110 K		
	<b>Calculated</b>	<b>Reported</b>	
<b>Volume</b>	4057.1(5) Å <sup>3</sup>	4057.1(5) Å <sup>3</sup>	
<b>Space group</b>	C 2/c	C 1 2/c 1	
<b>Hall group</b>	-C 2yc	-C 2yc	
<b>Molecular formula</b>	C <sub>48</sub> H <sub>70</sub> N <sub>2</sub>	C <sub>48</sub> H <sub>70</sub> N <sub>2</sub>	
<b>Sum formula</b>	C <sub>48</sub> H <sub>70</sub> N <sub>2</sub>	C <sub>48</sub> H <sub>70</sub> N <sub>2</sub>	
<b>Mr</b>	675.06	675.06	
<b>Density, g cm<sup>-3</sup></b>	1.105	1.105	
<b>Z</b>	4	4	
<b>Mu (mm<sup>-1</sup>)</b>	0.063	0.063	
<b>F000</b>	1488.0	1488.0	
<b>F000'</b>	1488.47		
<b>h,k,lmax</b>	32, 13, 24	32, 13, 24	
<b>Nref</b>	4660	4655	
<b>T<sub>min</sub>,T<sub>max</sub></b>	0.979, 0.990	0.454,0.482	
<b>T<sub>min</sub>'</b>	0.979		

Correction method= # Reported T Limits: T<sub>min</sub>=0.454 T<sub>max</sub>=0.482

AbsCorr = MULTI-SCAN

Data completeness= 0.999

Theta(max)= 27.498

R(reflections)= 0.0376 (4049)

wR2(reflections)= 0.0989 (4655)

S = 1.031

Npar= 230

**Table S4.** Crystal data and structure refinement for **1b\_PS**

<b>Bond precision:</b>	C-C = 0.0037 Å	Wavelength=1.54178	
<b>Cell:</b>	a= 13.0055 (5) Å	b=13.0942 (5) Å	c=18.4103 (7) Å
	alpha=91.925 (2) °	beta=92.264 (2) °	gamma=116.058 (1) °
<b>Temperature:</b>	110 K		
	<b>Calculated</b>	<b>Reported</b>	
<b>Volume</b>	2809.78 (19) Å <sup>3</sup>	2809.78 (19) Å <sup>3</sup>	
<b>Space group</b>	P -1	P -1	
<b>Hall group</b>	-P 1	-P 1	
<b>Molecular formula</b>	C <sub>52</sub> H <sub>48</sub> N <sub>2</sub> O <sub>4</sub> , 3.8(C H <sub>2</sub> Cl <sub>2</sub> ), Br	Br, 2(C <sub>26</sub> H <sub>24</sub> NO <sub>2</sub> ), 3.8(CH <sub>2</sub> Cl <sub>2</sub> )	
<b>Sum formula</b>	C <sub>55.80</sub> H <sub>55.60</sub> BrCl <sub>7.60</sub> N <sub>2</sub> O <sub>4</sub>	C <sub>55.80</sub> H <sub>55.60</sub> BrCl <sub>7.60</sub> N <sub>2</sub> O <sub>4</sub>	
<b>Mr</b>	1167.54	1167.55	
<b>Density, g cm<sup>-3</sup></b>	1.380	1.380	
<b>Z</b>	2	2	
<b>Mu (mm<sup>-1</sup>)</b>	4.686	4.686	

<b>F000</b>	1201.2	1201.0
<b>F000'</b>	1207.88	
<b>h,k,lmax</b>	15, 15, 22	15, 15, 22
<b>Nref</b>	10664	10664
<b>T<sub>min</sub>,T<sub>max</sub></b>	0.391, 0.606	0.136, 0.351
<b>T<sub>min</sub>'</b>	0.108	

Correction method= # Reported T Limits: T<sub>min</sub>=0.136 T<sub>max</sub>=0.351

AbsCorr = MULTI-SCAN

Data completeness= 0.998

Theta(max)= 70.153

R(reflections)= 0.0523 (10245)

wR2(reflections)= 0.1420 (10644)

S = 1.030

Npar= 725

### 13. Grazing-Incidence Wide-Angle X-Ray Scattering

Grazing-incidence wide-angle X-ray scattering (GIWAXS) measurements were carried out in Sector 8-ID-E at the Advanced Photon Source, Argonne National Laboratory.<sup>7</sup> Beamline 8-ID-E operates at an energy of 10.92 keV and the images were collected from a Pilatus 1MF camera (Dectris), with two exposures for different vertical positions of the detector. After flat field correction for detector nonuniformity, the images are combined to fill in the gaps for rows at the borders between modules, inactive pixels at the center were left dark. Using the GIXSGUI package<sup>11</sup> for MATLAB (Mathworks), data are corrected for X-ray polarization, detector sensitivity and geometrical solid-angle. Solid-state samples were prepared by spin-casting (5 mg mL<sup>-1</sup> in THF, **1a\_PB**, **P1a\_PB** mixed with 10 equivalents of HCl) thin films of **1a\_PS**, **P1a\_PS** on UV-Ozone cleaned bare n-type Si wafers with 300 nm SiO<sub>2</sub> at 1000 RPM for 1 minute. The as-

cast samples were measured directly and the annealed samples were thermally treated (100 °C, 10 min) before the measurements.

Both **1a\_PS** (Figure S15, left) and **P1a\_PS** (Figure S15, right) exhibited amorphous characters.

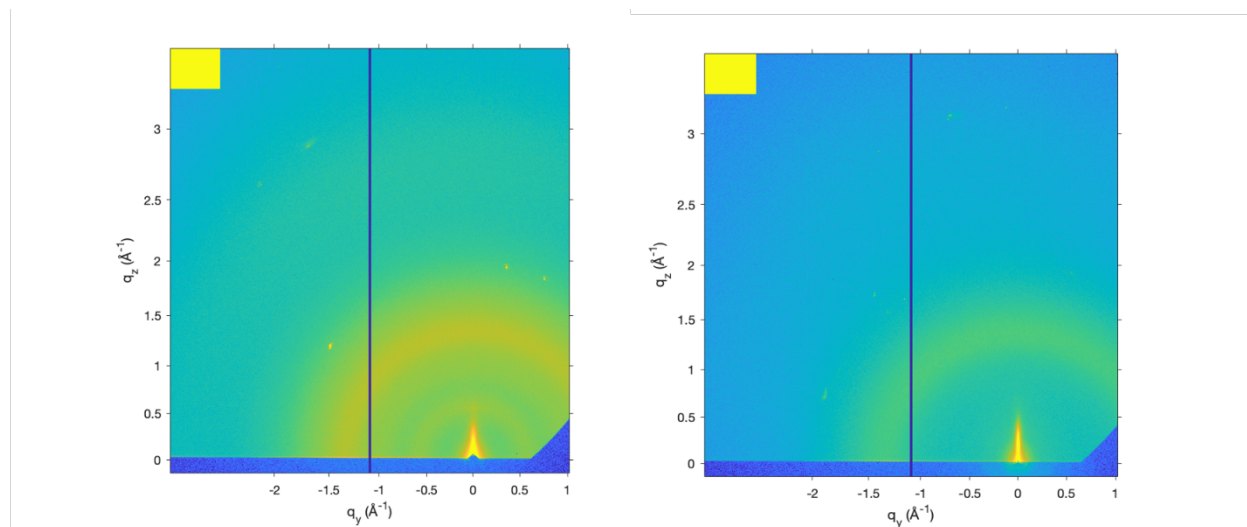


**Figure S17.** Grazing-incidence Wide-angle X-ray Scattering (GIWAXS) spectra of **1a\_PS** (left) and **P1a\_PS** (right) spin-coated films on silicon wafer after annealing.

## 14. NMR Spectra

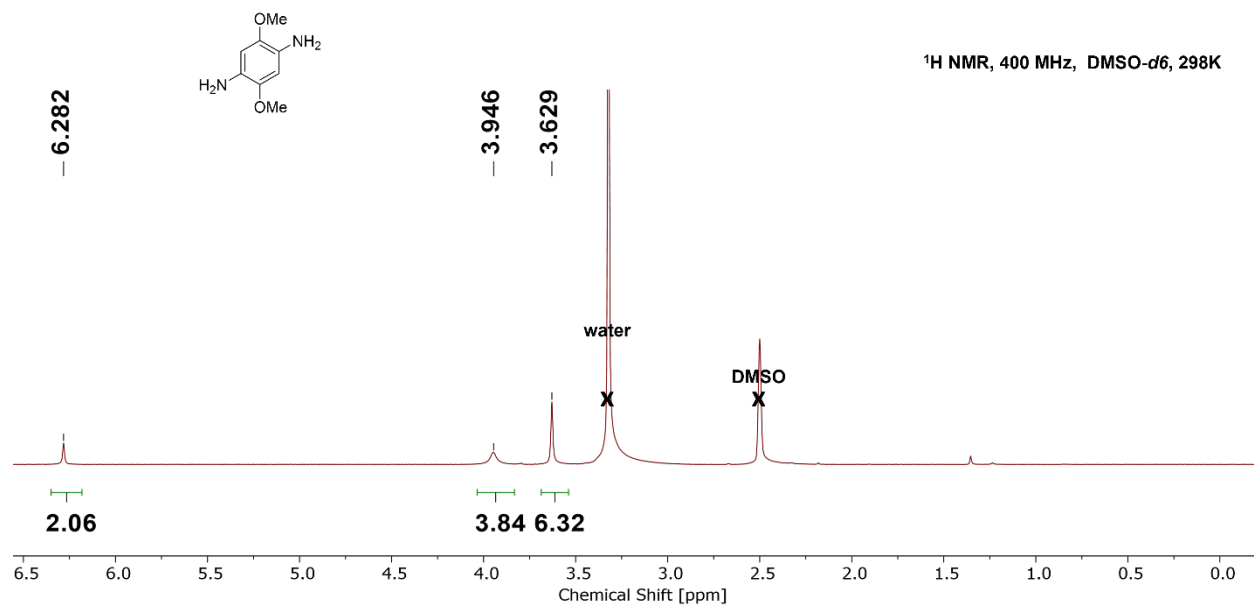


Figure S18. <sup>1</sup>H NMR of 2a.

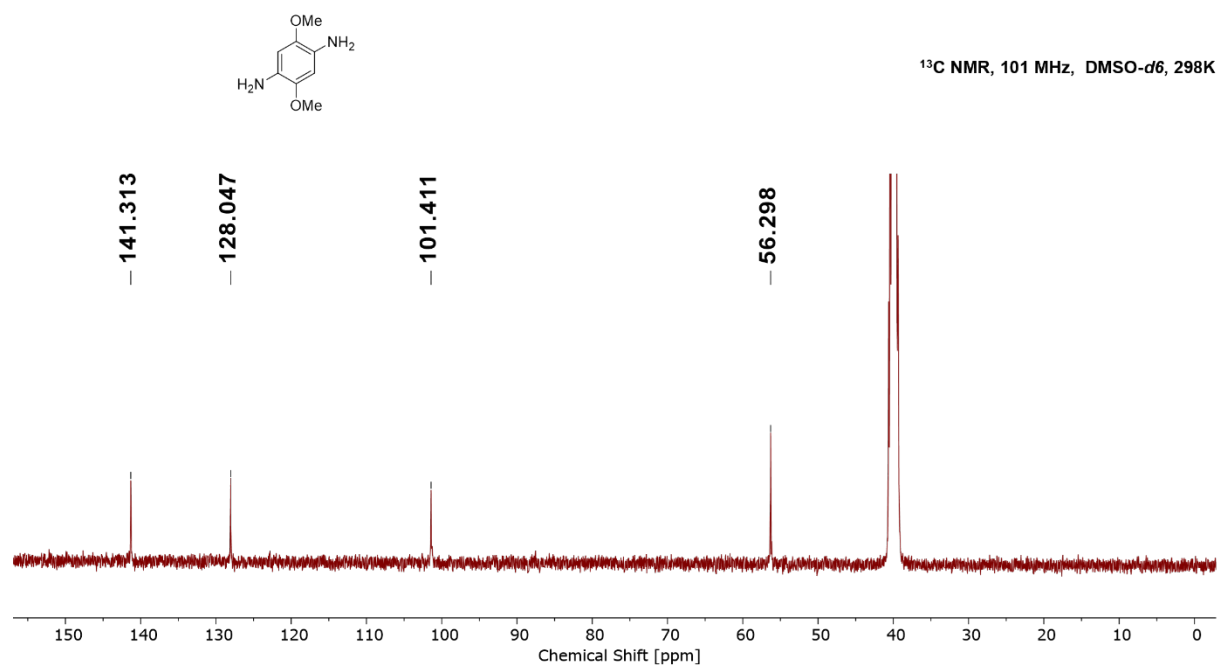
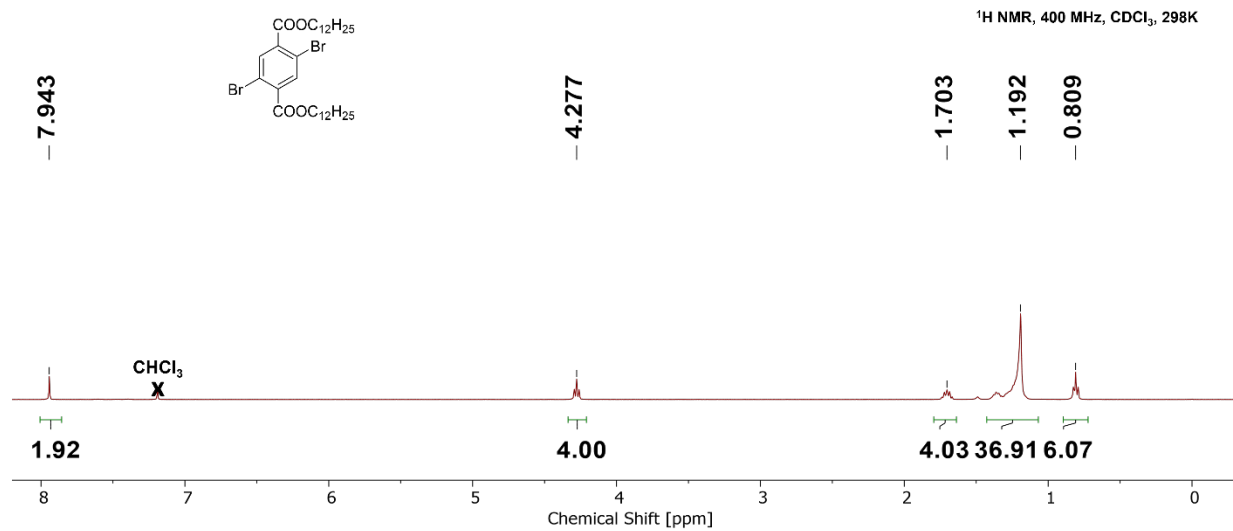
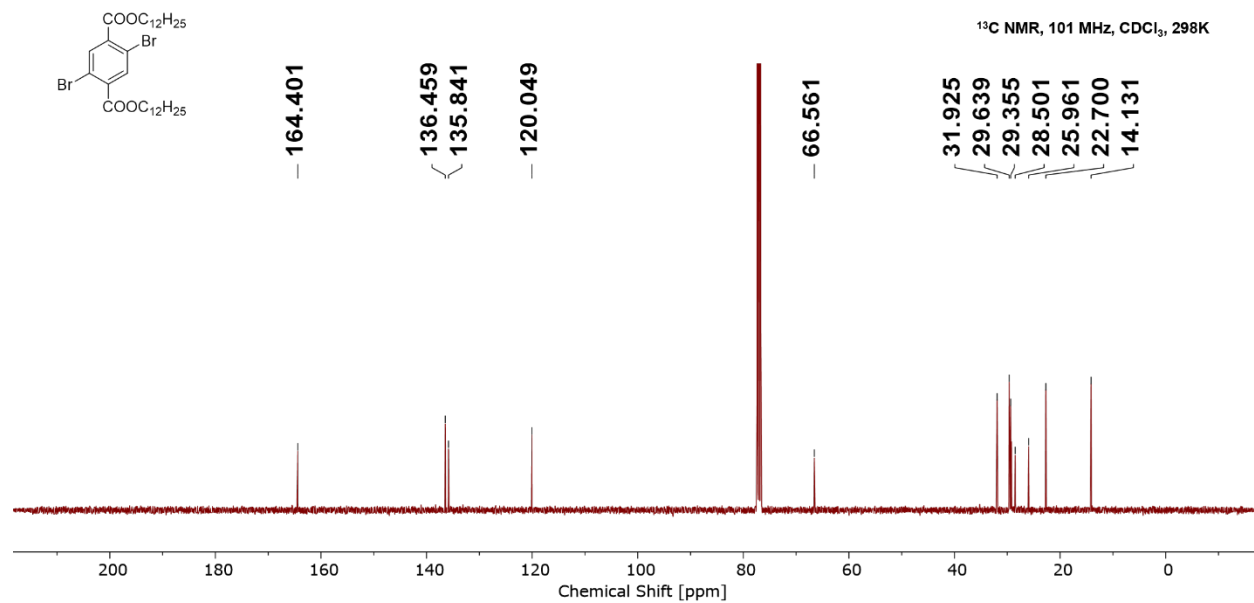


Figure S19. <sup>13</sup>C NMR of 2a.



**Figure S20.** <sup>1</sup>H NMR of **3**.



**Figure S21.** <sup>13</sup>C NMR of **3**.

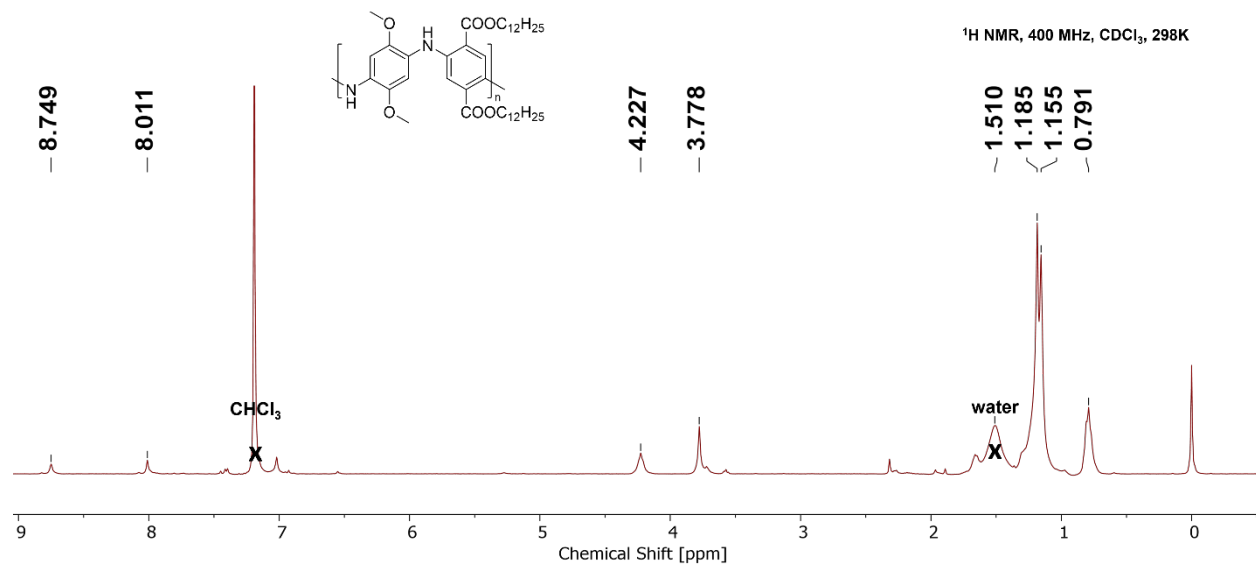


**Figure S22.** <sup>1</sup>H NMR of P2a.

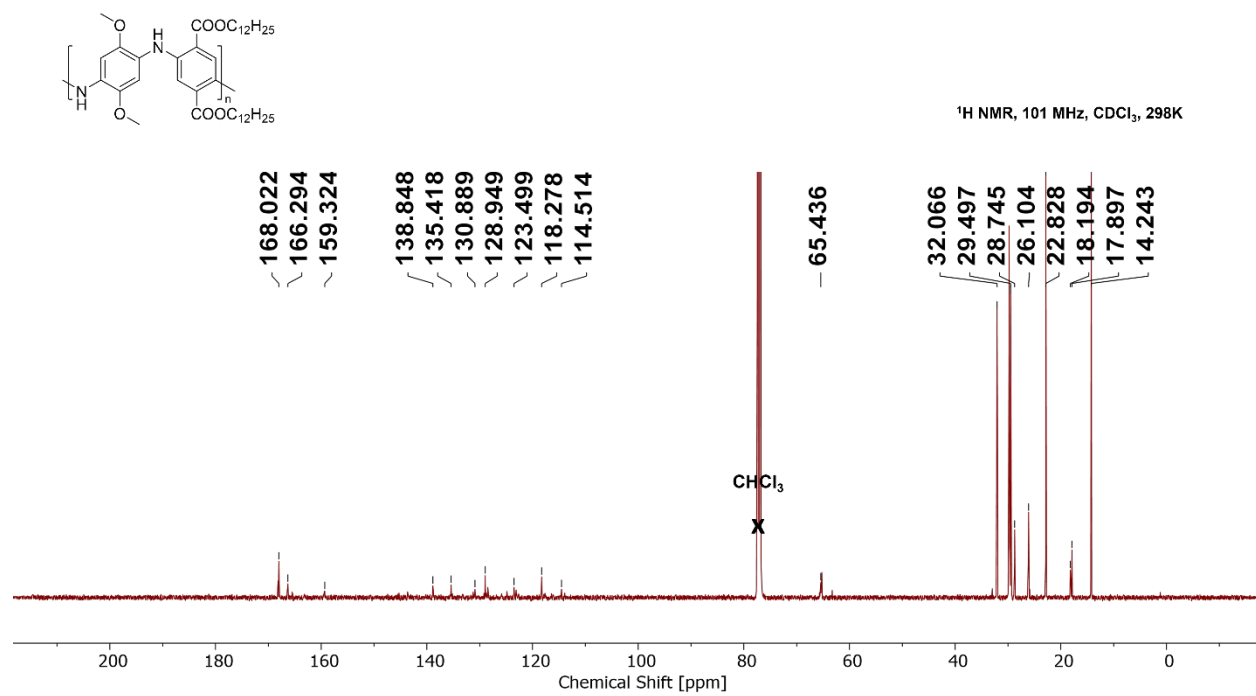


**Figure S23.** <sup>13</sup>C NMR of P2a.

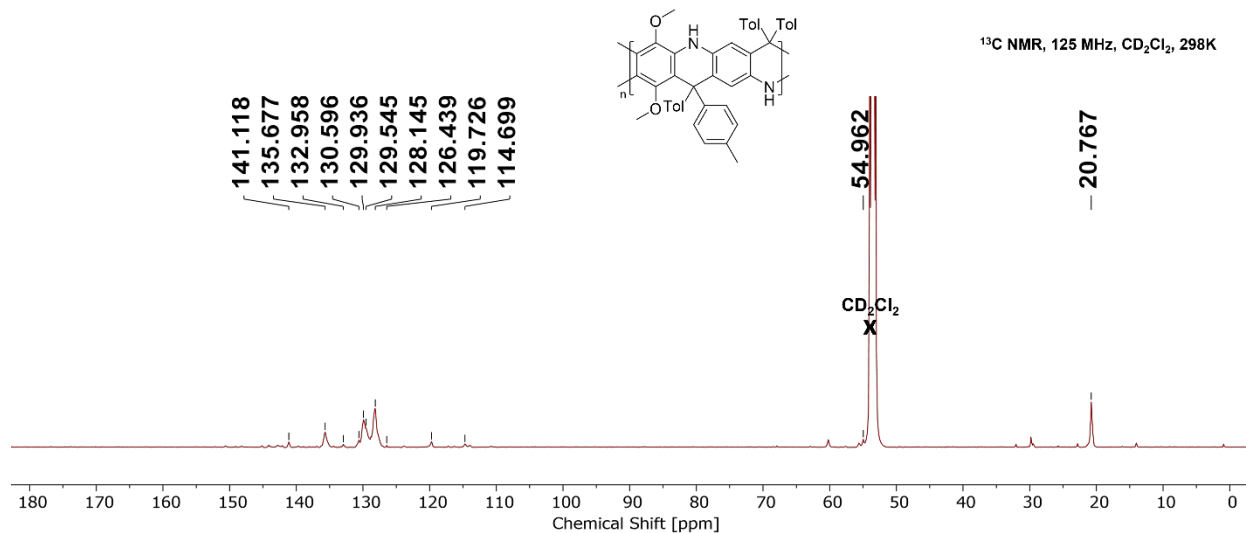


Figure S24. <sup>13</sup>C NMR of P1a\_LB.

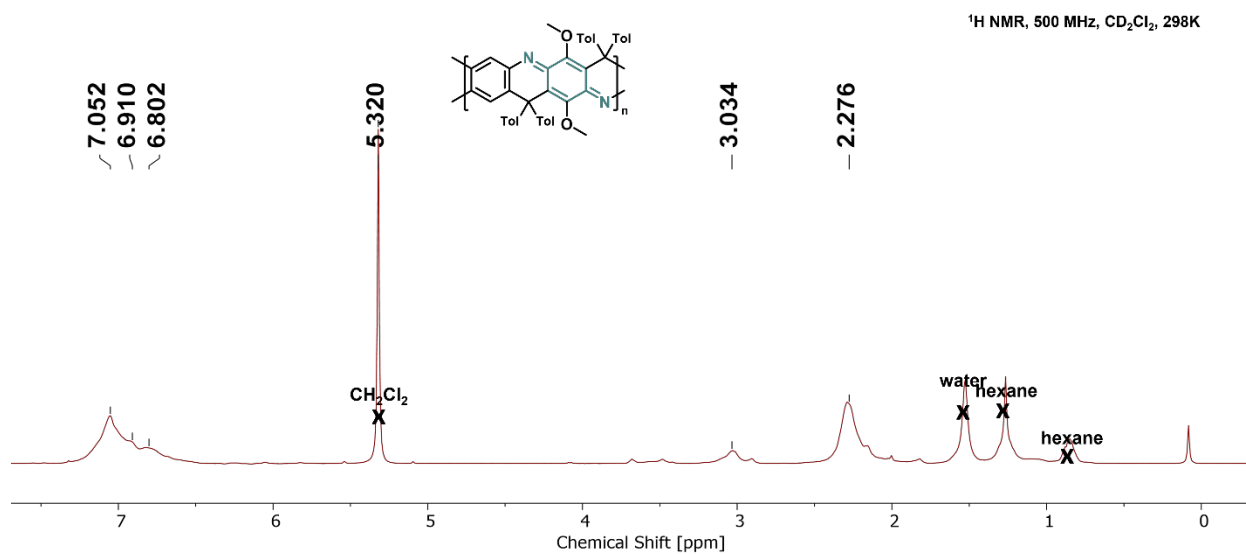


Figure S25. <sup>1</sup>H NMR of P1a\_PB.

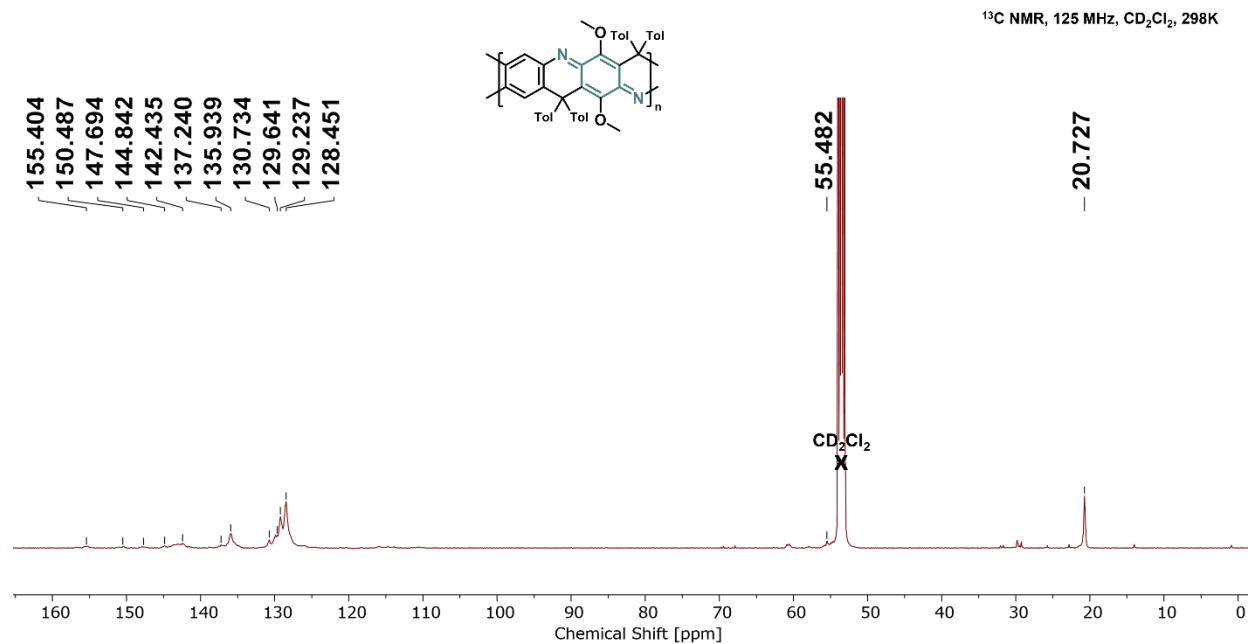


Figure S26. <sup>13</sup>C NMR of P1a\_PB.

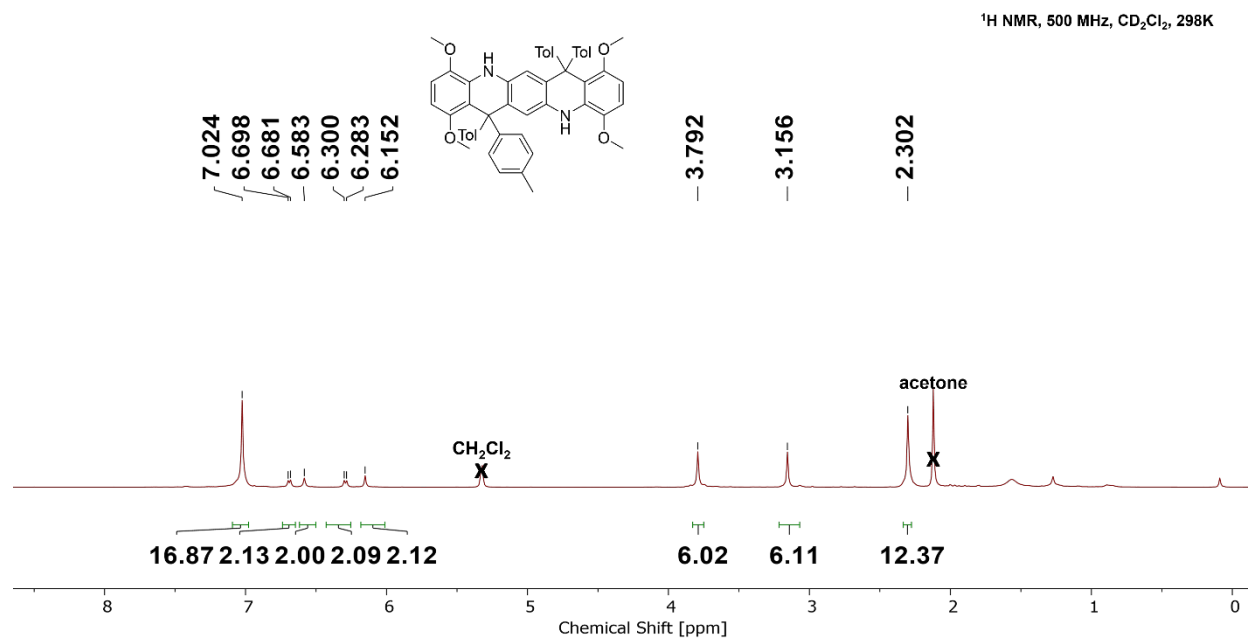


Figure S27. <sup>1</sup>H NMR of 1a\_LB.

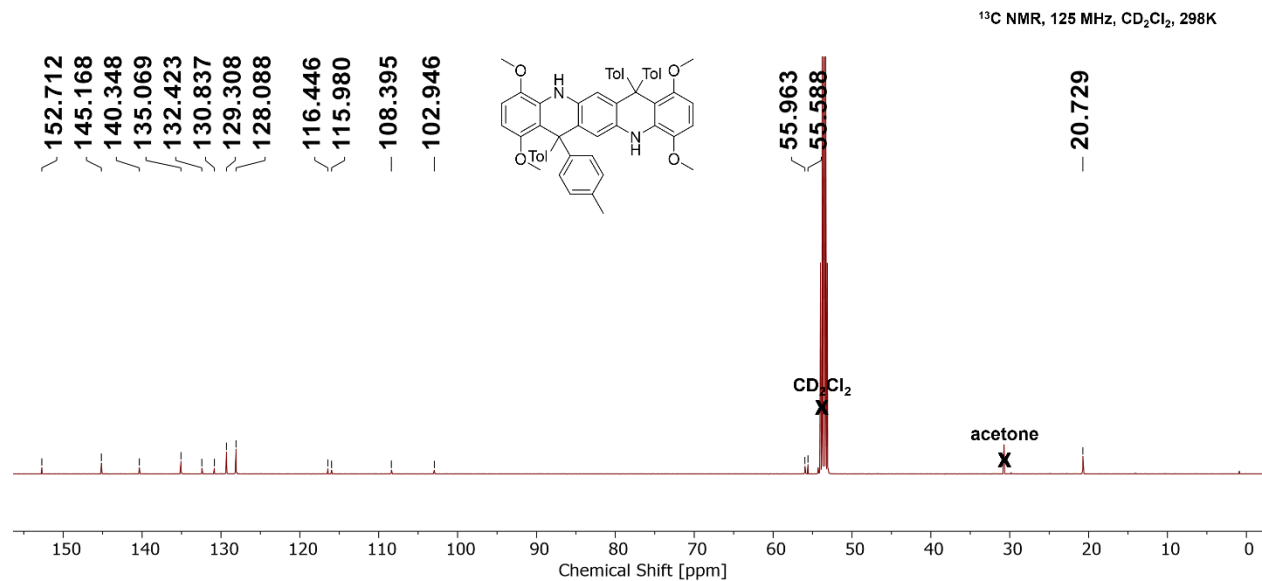


Figure S28. <sup>13</sup>C NMR of 1a\_LB.

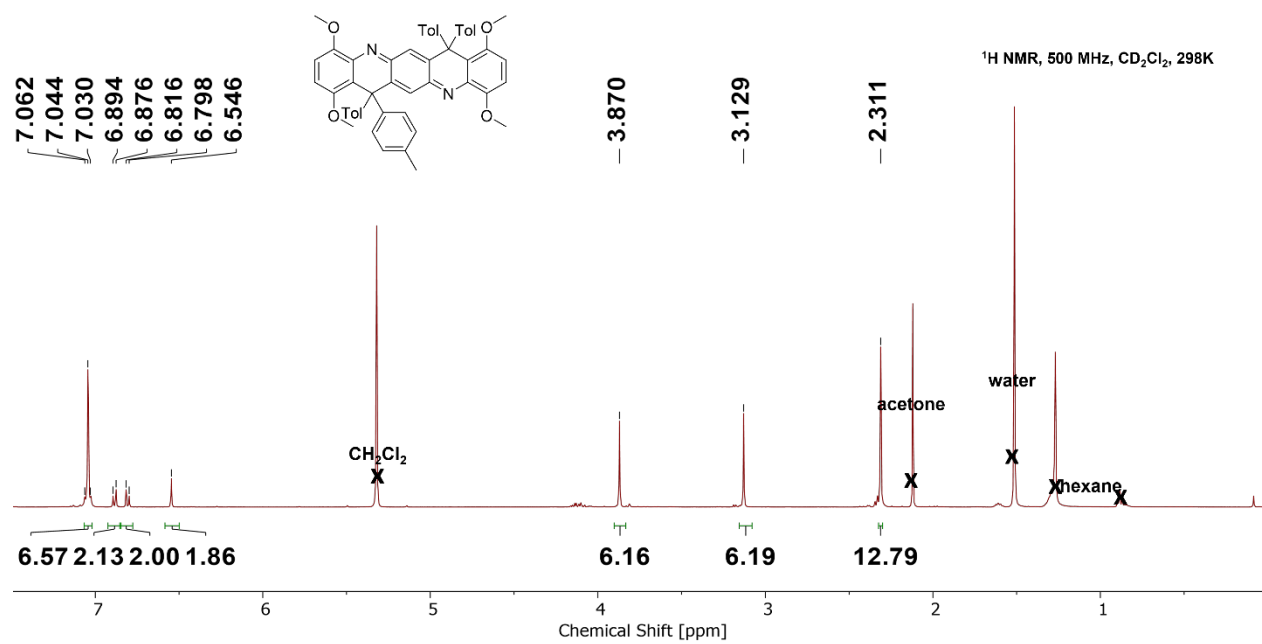
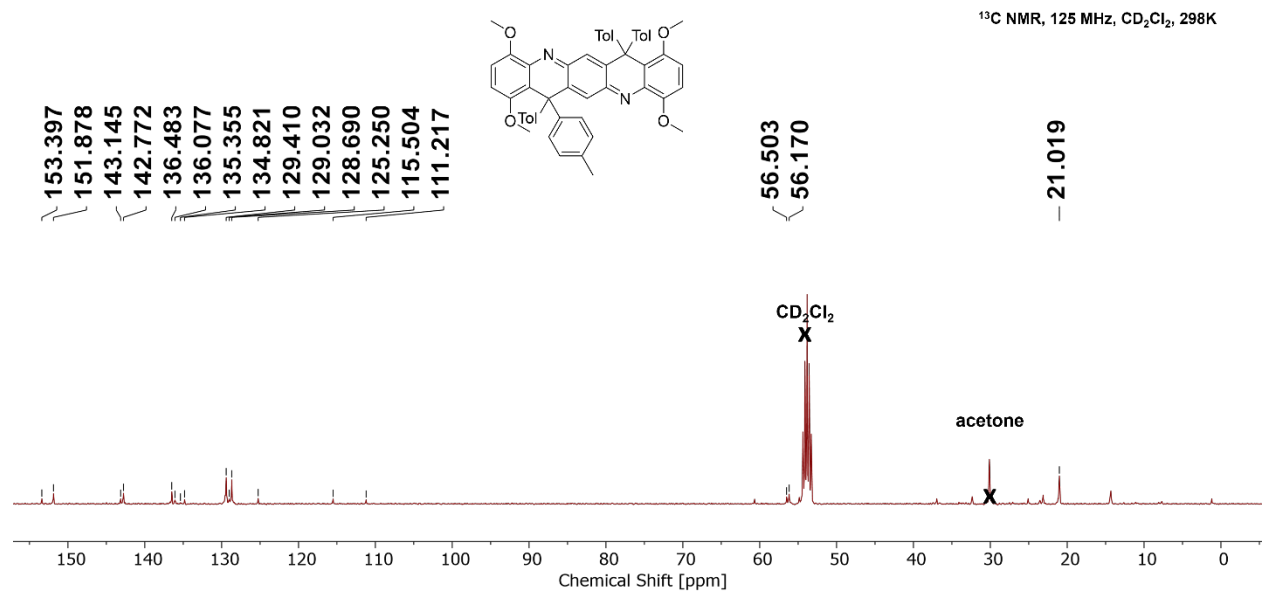
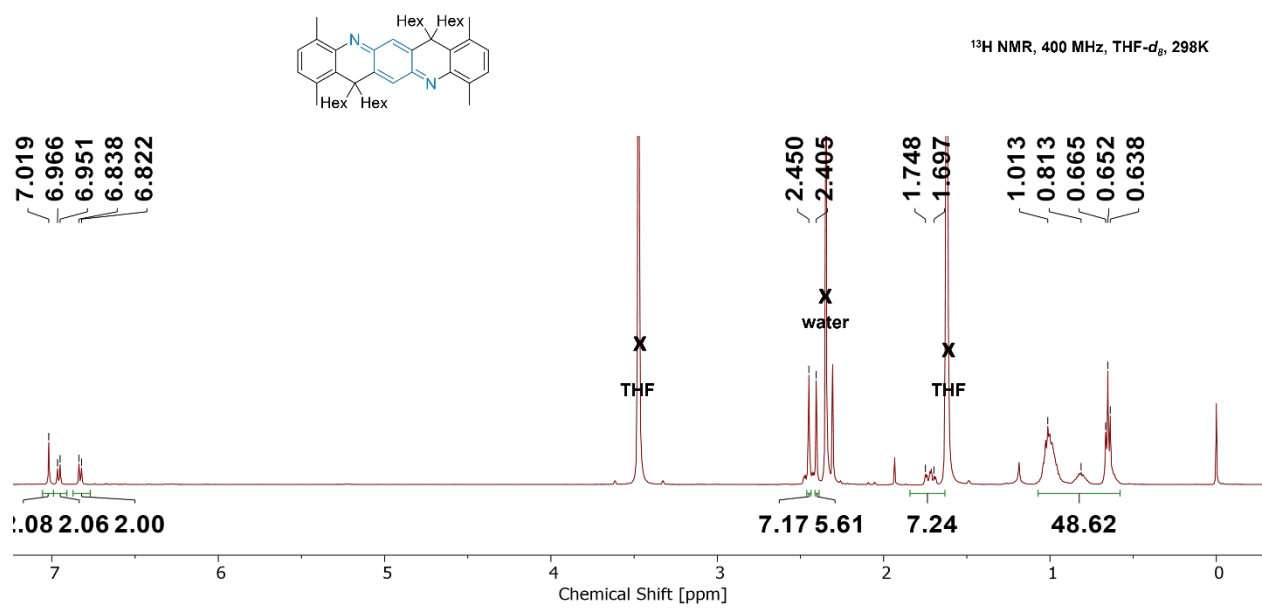


Figure S29. <sup>1</sup>H NMR of 1a\_PB.



**Figure S30.** <sup>13</sup>C NMR of **1a\_PB**.



**Figure S31.** <sup>1</sup>H NMR of **1b\_PB**.

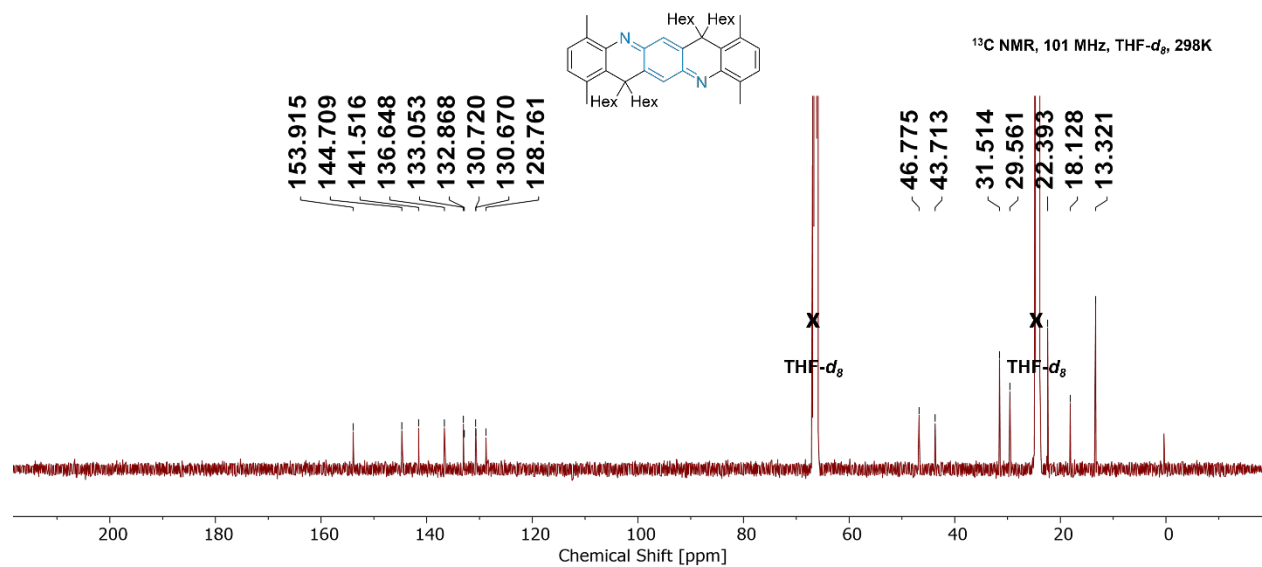


**Figure S32.** <sup>13</sup>C NMR of **1b**\_PB.

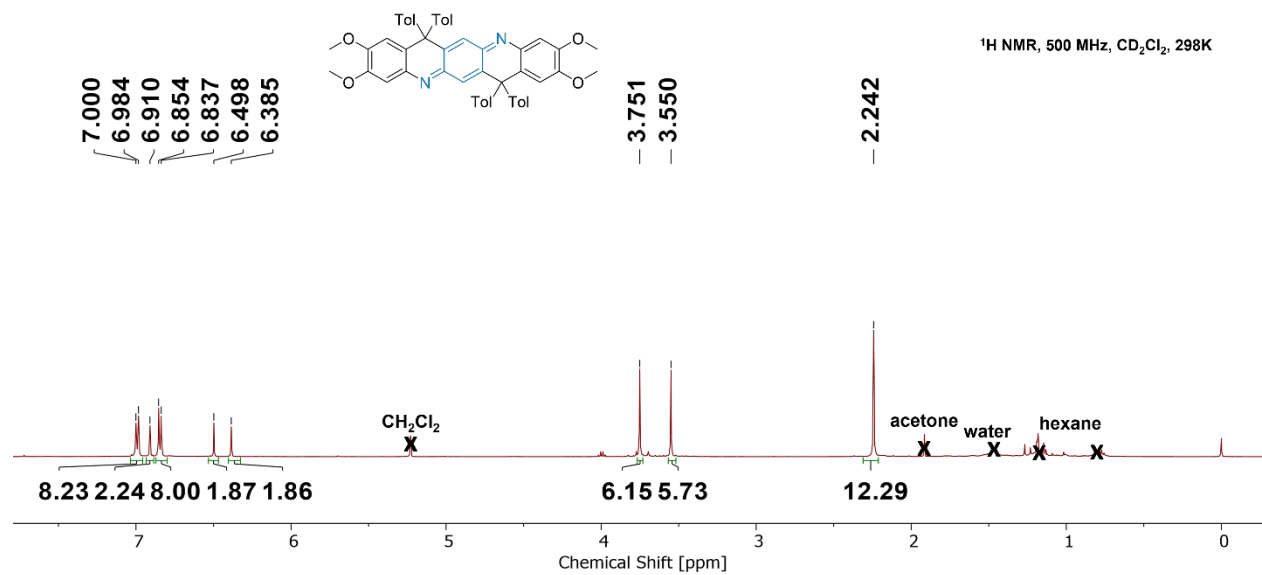


**Figure S33.** <sup>1</sup>H NMR of **1c**\_PB.

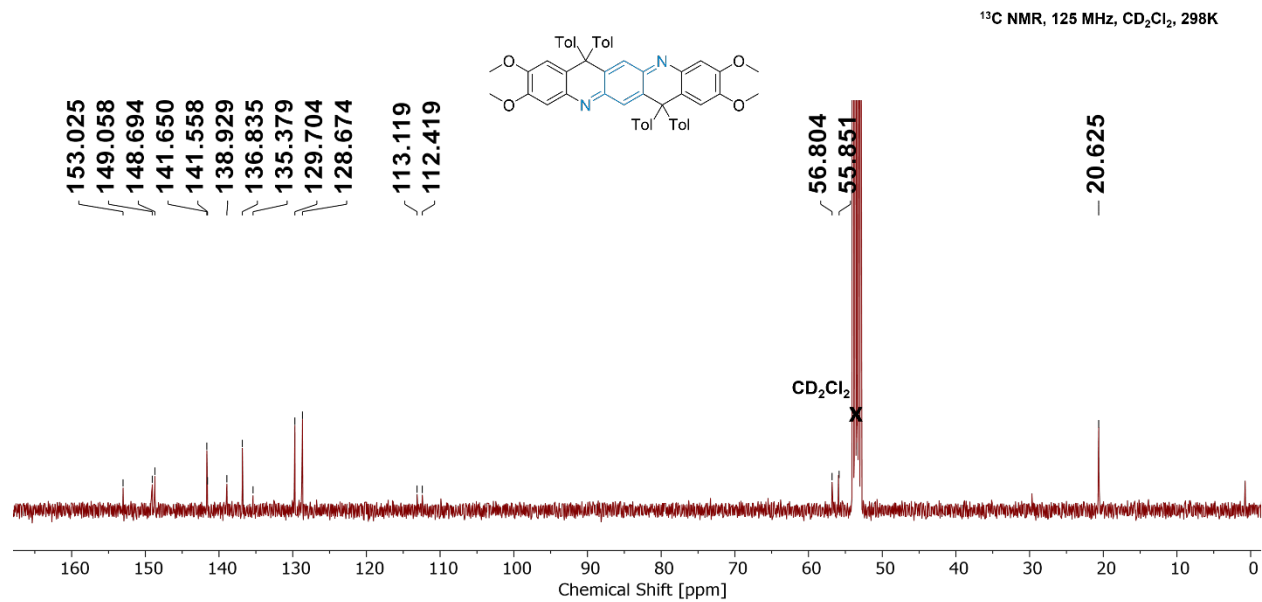


Figure S34. <sup>13</sup>C NMR of 1c\_PB.

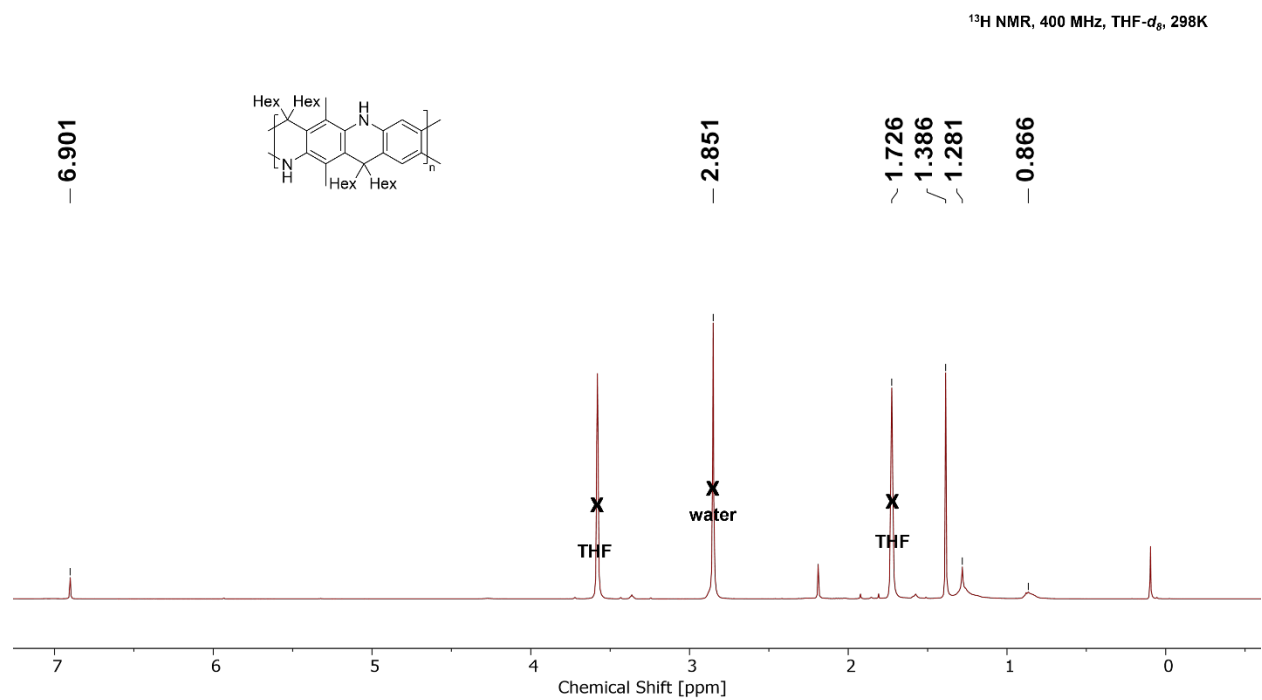
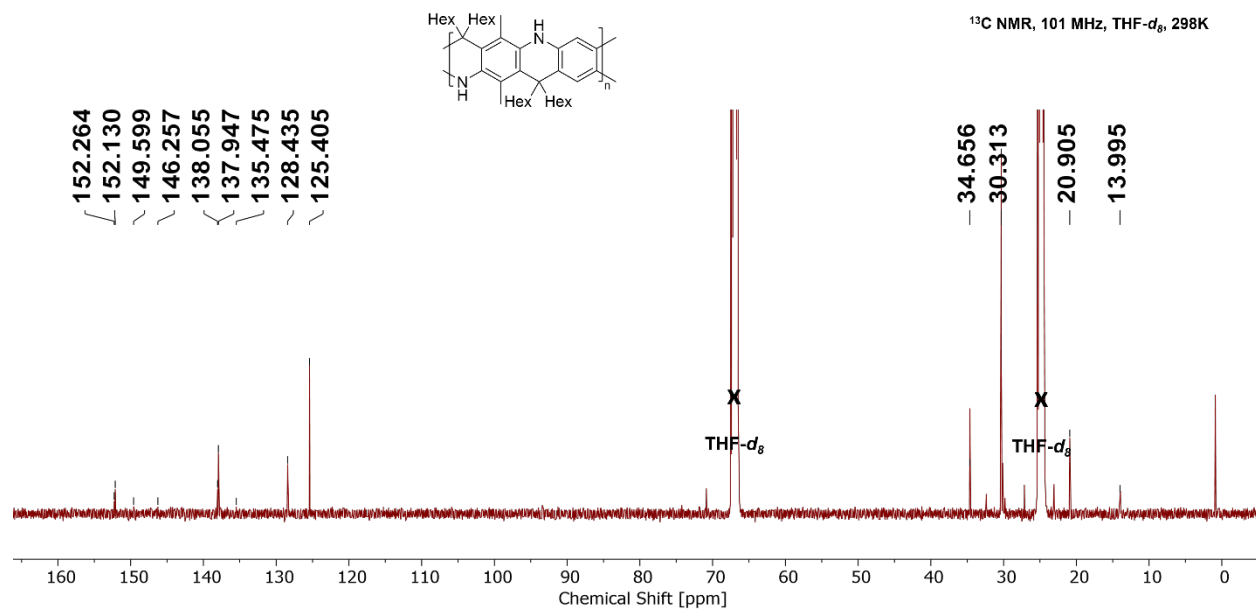
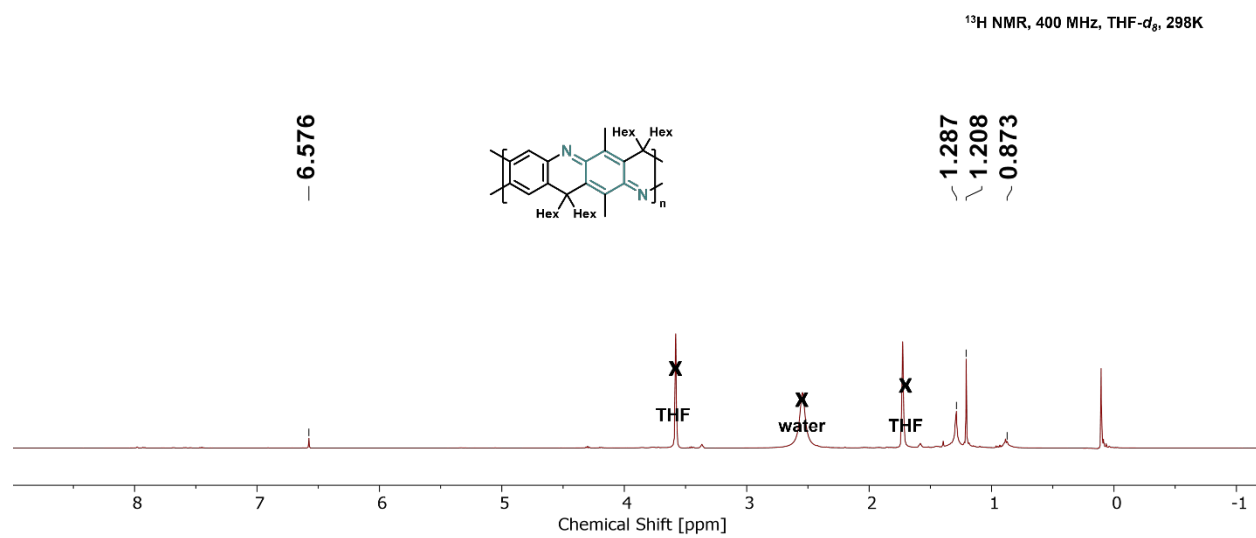


Figure S35. <sup>1</sup>H NMR of P1b\_LB.



**Figure S36.** <sup>13</sup>C NMR of P1b\_LB.



**Figure S37.** <sup>1</sup>H NMR of P1b\_PB.

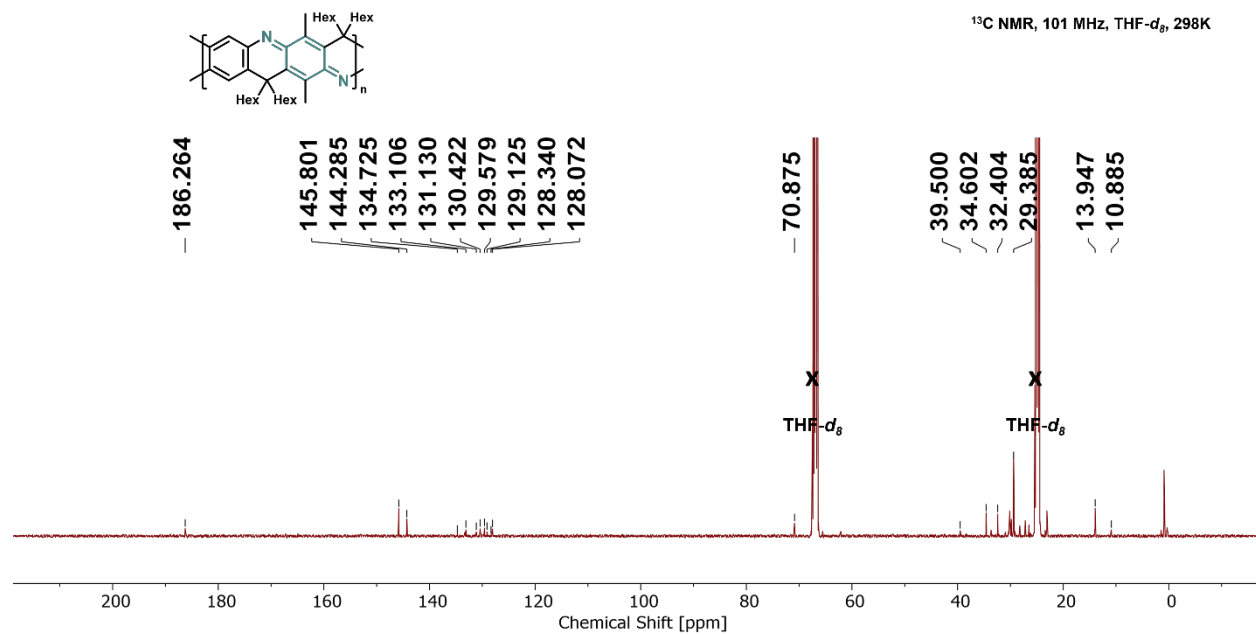


Figure S38. <sup>13</sup>C NMR of P1b\_PB.

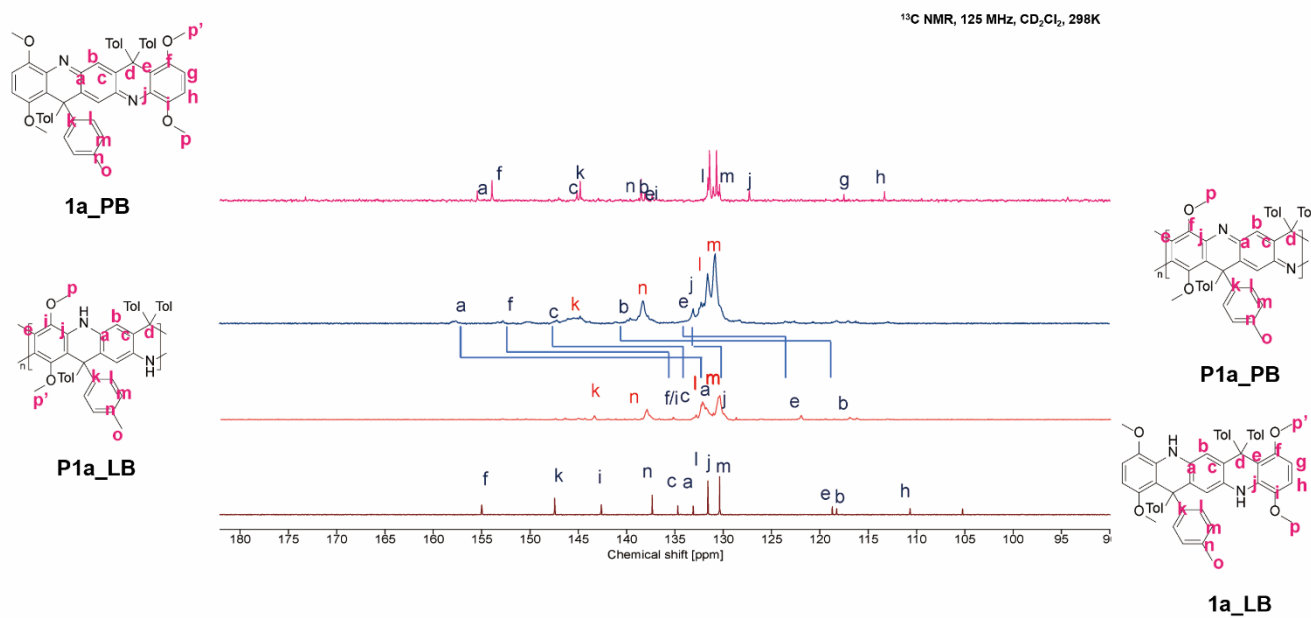
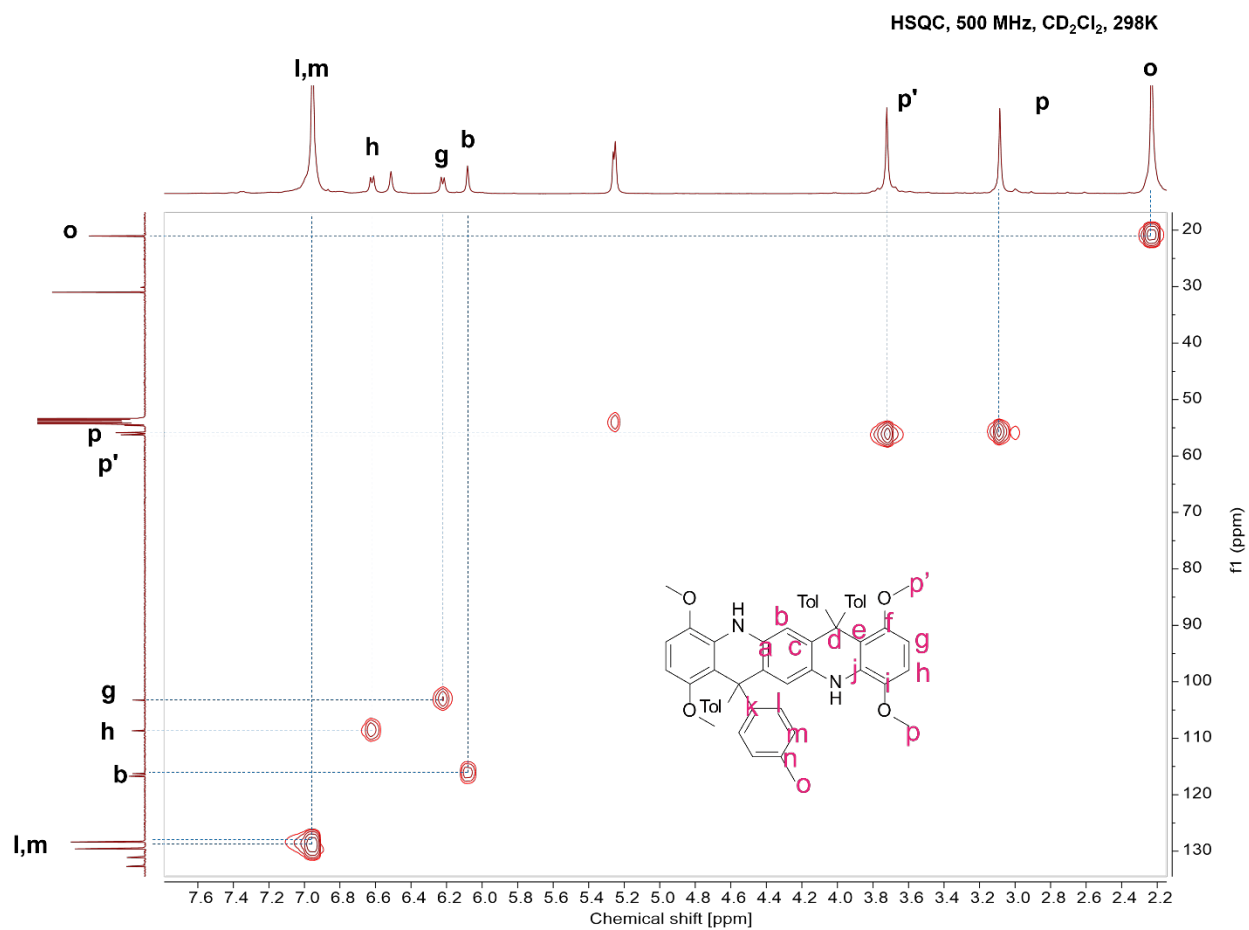


Figure S39. <sup>13</sup>C NMR comparison: 1a\_PB, P1a\_PB, P1a\_LB, 1a\_LB.



**Figure S40.** HSQC NMR of **1a\_LB**.

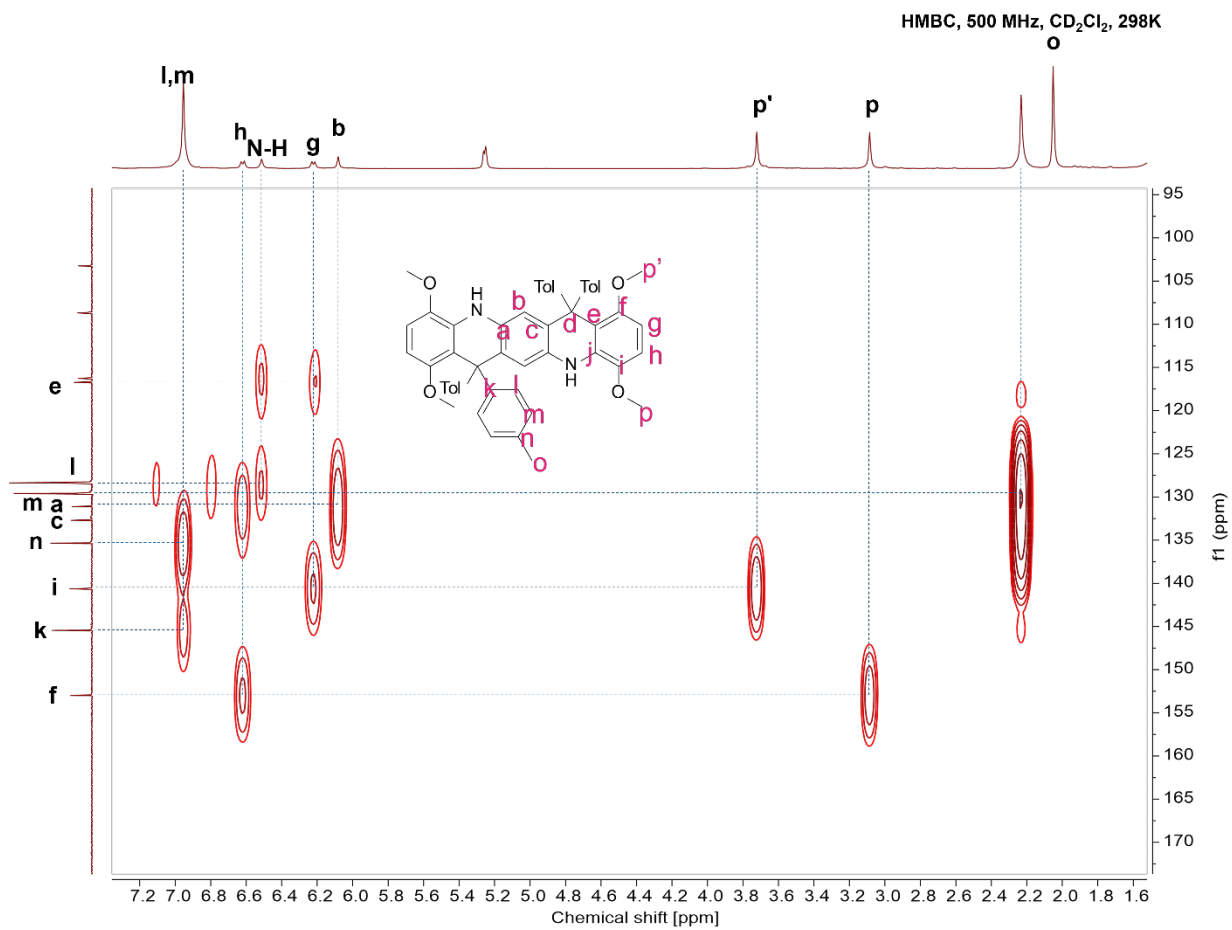


Figure S41. HMBC NMR of 1a\_LB.



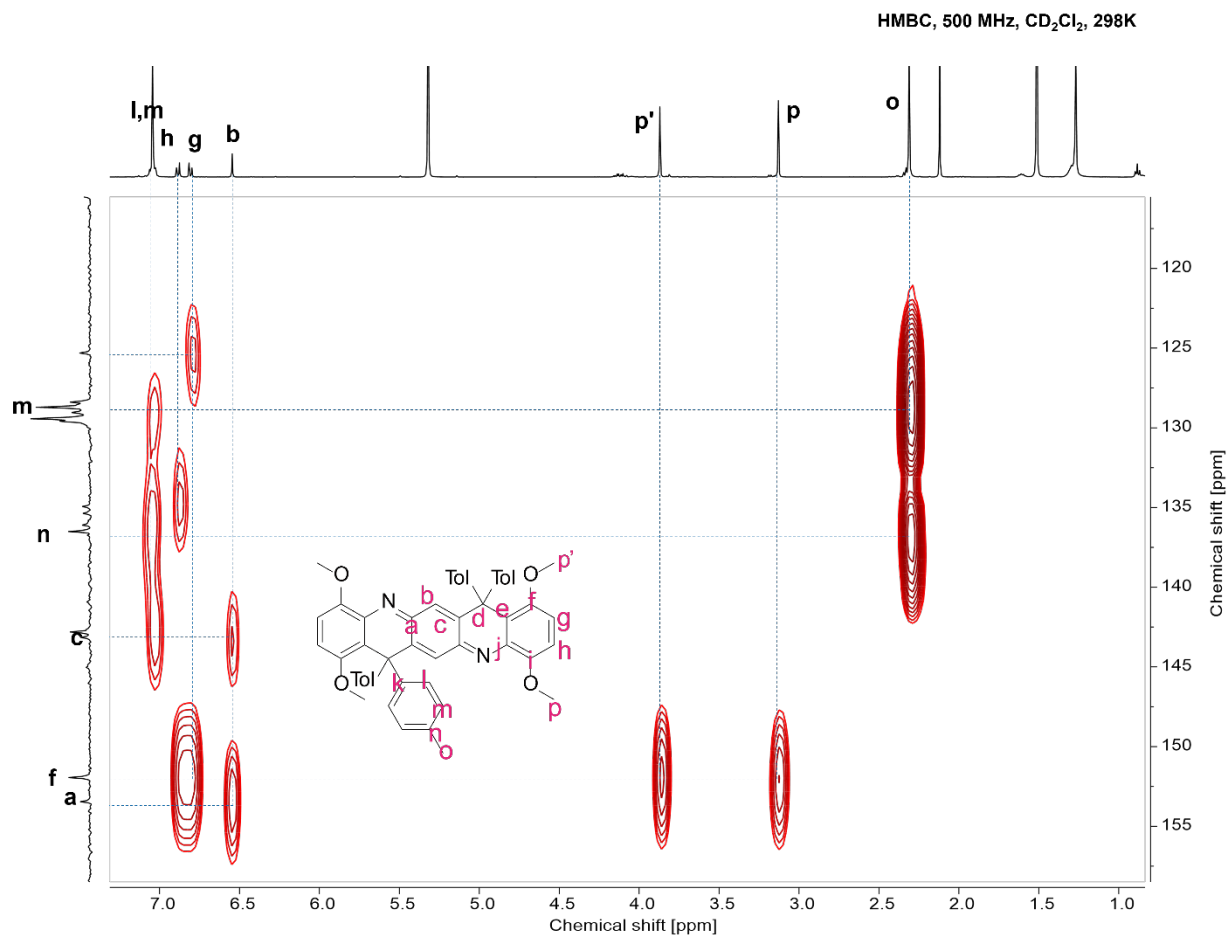
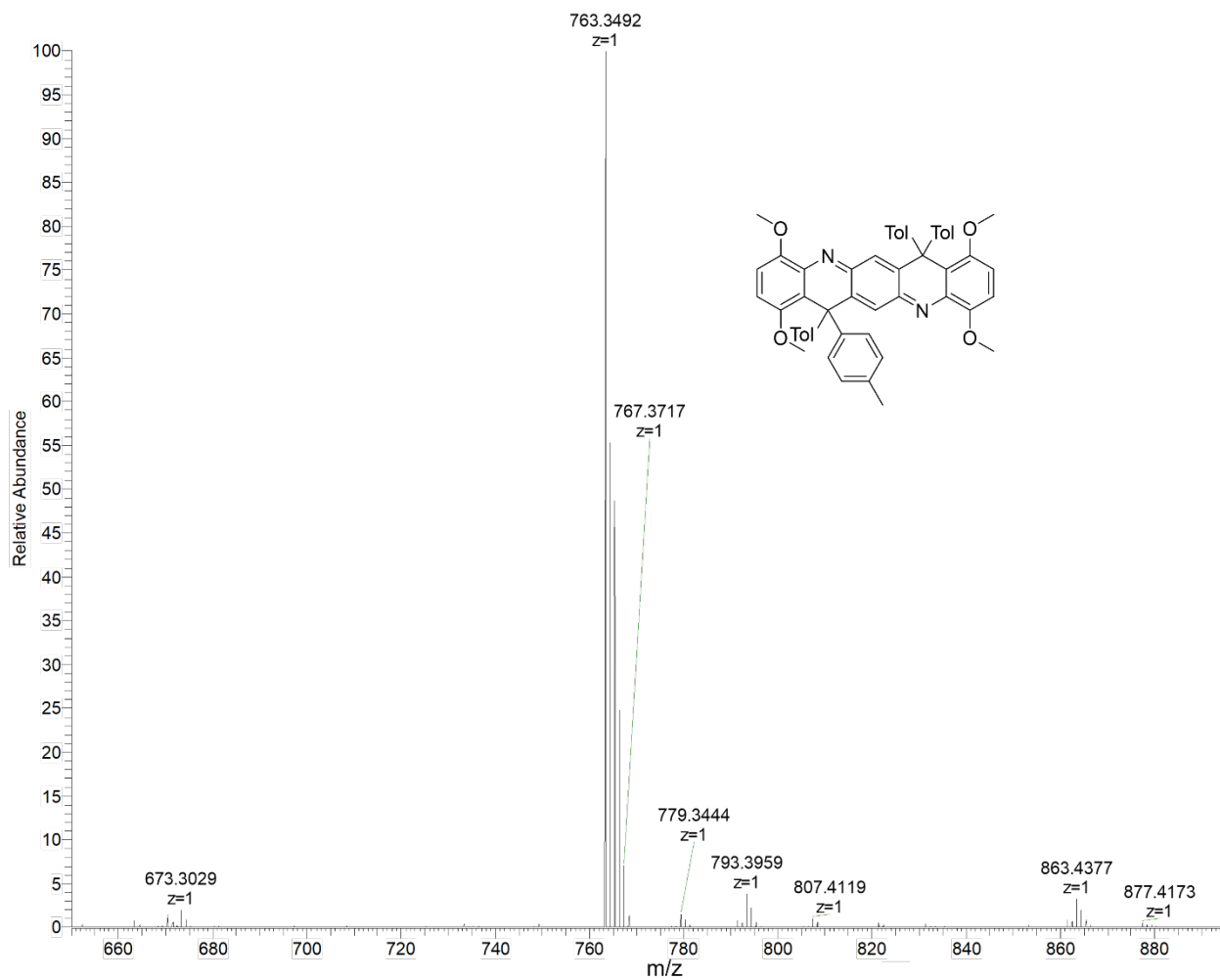
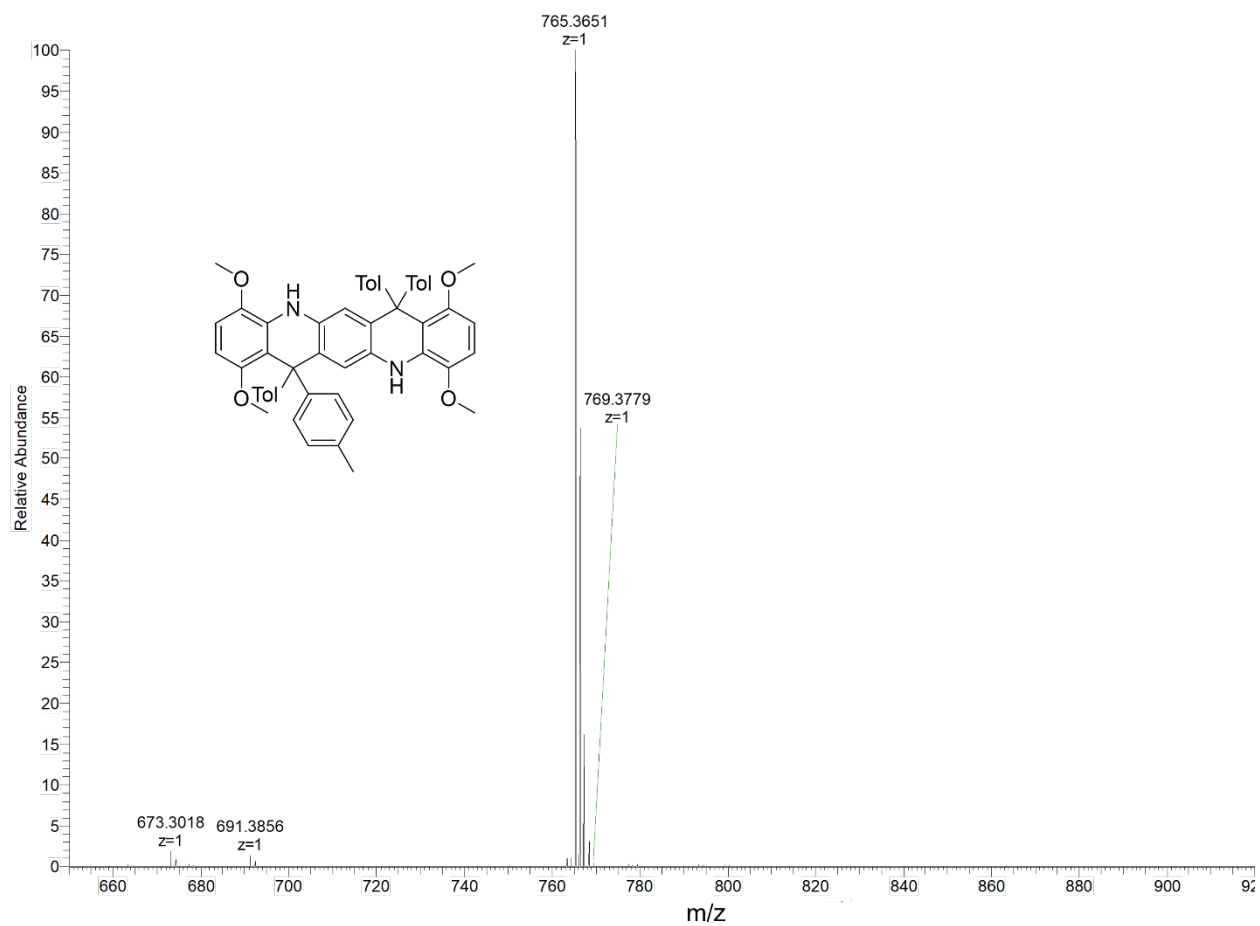


Figure S43. HMBC NMR of **1a\_PB**.

## 15. Mass Spectra



**Figure S44.** APCI-MS spectrum of 1a\_PB.



**Figure S45.** APCI-MS spectrum of 1a\_LB.

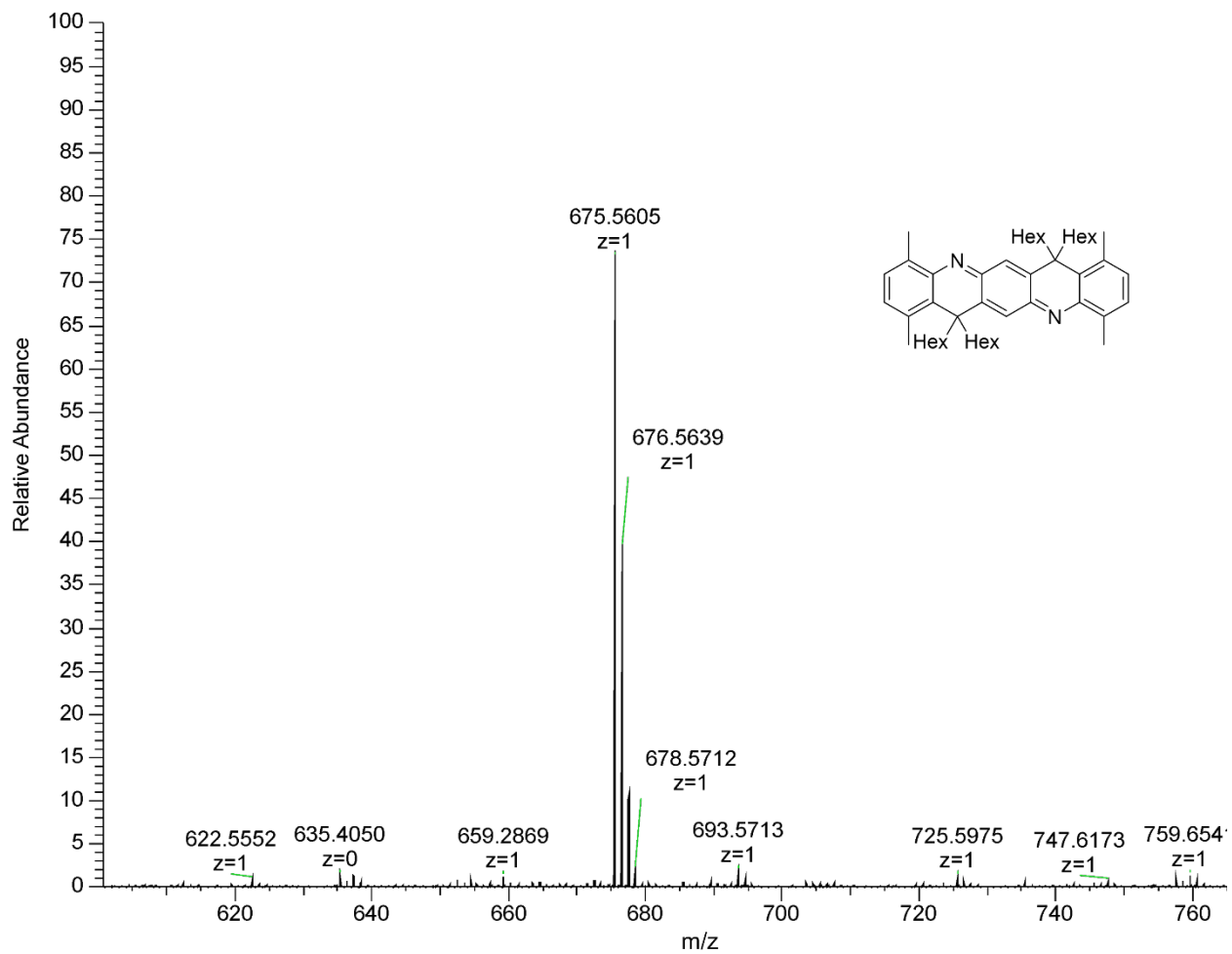


**Figure S46.** APCI-MS spectrum of 1b\_PB.

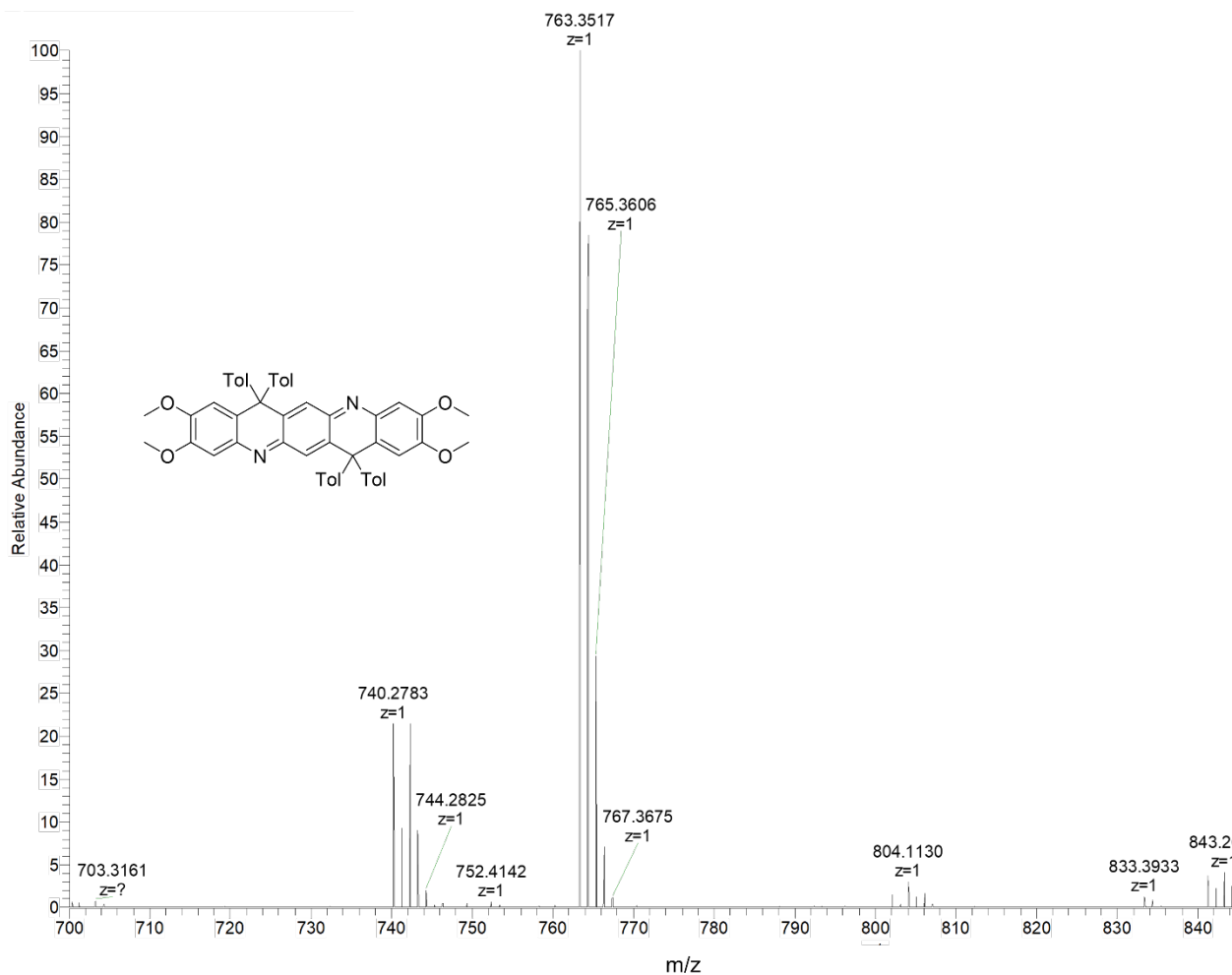


**Figure S47.** APCI-MS spectrum of **1c\_PB**.

## References

1. J. Wu, Fang, W.-Y. Lu, J.-L. Hou, C. Li, Z.-Q. Wu, X.-K. Jiang, Z.-T. Li and Y.-H. Yu, *J. Org. Chem.*, 2007, **72**, 2897-2905.
2. M. Otaki, R. Kumai, H. Sagayama and H. Goto, *Macromolecules*, 2019, **52**, 2340-2348.
3. <http://supramolecular.org>.
4. P. Thordarson, *Chem. Soc. Rev.*, 2011, **40**, 1305-1323.
5. K. C. Felton, J. G. Rittig and A. A. Lapkin, *Chemistry-Methods*, 2021, **1**, 116-122.
6. M. D. McKay, R. J. Beckman and W. J. Conover, *Technometrics*, 2000, **42**, 55-61.

7. Z. Jiang, X. Li, J. Strzalka, M. Sprung, T. Sun, A. R. Sandy, S. Narayanan, D. R. Lee and J. Wang, *J. Synchrotron Radiat.*, 2012, **19**, 627-636.